THESIS

Immunohistochemical expression of HBp17/FGFBP-1, FGF-1, FGF-2, CD34, p53, pRB, and Ki67 in Ameloblastomas

NGUYEN THANH TUNG

Ph.D THESIS

Immunohistochemical expression of HBp17/FGFBP-1, FGF-1, FGF-2, CD34, p53, pRB, and Ki67 in Ameloblastomas

by

NGUYEN THANH TUNG

Department of Molecular Oral Medicine and Maxillofacial Surgery

Graduate School of Biomedical Sciences

Hiroshima University

2013

A Thesis Submitted in Partial Fulfilment of the Requirements for the Degree of Doctor Philosophy (Ph.D) in Molecular Oral Medicine and Maxillofacial Surgery

The studies in this thesis were performed by under supervision of Prof. Tetsuji Okamoto from Department of Molecular Oral Medicine and Maxillofacial Surgery, Graduate Institute of Biomedical & Health Sciences, Hiroshima University

Principal Academic Advisor: Professor Tetsuji Okamoto

Department of Molecular Oral Medicine and Maxillofacial Surgery, Division of Frontier Medical Science, Graduate Institute of Biomedical & Health Sciences, Hiroshima University.

Telephone: +81-82-257-5665

Fax: + 81-82-257-5669

E-mail address: tetsuok@hiroshima-u.ac.jp

Academic Advisor: Professor Takashi Takata

Department of Oral Maxillofacial Pathology, Graduate Institute of Biomedical & Health Sciences, Hiroshima University.

Academic Advisor: Professor Hidemi Kurihara

Department of Periodontal Medicine, Graduate Institute of Biomedical & Health Sciences, Hiroshima University.

Advisor: Dr. Yasuto Fukui

Department of Molecular Oral Medicine and Maxillofacial Surgery, Division of Frontier Medical Science, Graduate School of Biomedical & Health Sciences, Hiroshima University.

Acknowledgment

Foremost, I would like to express my deep gratitude to Principal Academic Advisor Professor Tetsuji Okamoto and my supervisor, Dr. Yasuto Fukui, for their patient guidance, enthusiastic encouragement and useful critiques during the process of my research.

I would also like to thank Professor Takashi Takata and Professor Hidemi Kurihara for being the advisors in my study, and also Professor Takashi Uchida, Professor Masaru Sugiyama and Dr. Shigeaki Toratani for their advice and reviewing my thesis.

My grateful thanks are also extended to Dr. Ikuko Ogawa and Ms. Keiko Banno, for their helps in doing the histopathologic diagnosis and doing the immunohistochemical staining as well as preparing the paraffine blocks, and to my best friends in Japan for sharing weal and woe as well.

I would like to acknowledge with much appreciation the collaboration between Hiroshima University and University of Medicine and Pharmacy at Ho Chi Minh City, especially the existence of Twinning Program between the two Universities and the Scholarship from the Ministry of Education, Culture, Sport, Science and Technology, Japan. Furthermore I would like to thank Professor

Hung Tu Hoang, Dr. Lan Anh Huynh, and Professor Phuong Hoai Lam for introducing me to the Twinning Programe as well for the support on the way.

In addition, many thanks to Dr. Thao Thi Nguyen and my colleagues at National Hospital of Odontostomatology who helped me collect the samples in Viet Nam.

Finally, I would like to express my deepest appreciation to my family, my close friends who are always by my side in the "depths of winter" and to all those who provided me the possibility and motivation to complete this PhD course.

Contents Page

1. Introduction

1. Introduction

Ameloblastoma, a benign odontogenic tumor, has locally invasive behavior with high recurrence rate. The etiological factors of ameloblastoma remain unknown, although it has been known for about two hundred years. Ameloblastoma was first reported by Cusack et al.[1] in 1827 and then Broca et al.[2] in 1868. Until 1885, Malassez[3] proposed the name “epithelioma adamentin” for solid/multicystic ameloblastoma and the term ameloblastoma which is currently used was re-named by Ivey and Churchill[4] in 1930. The several etiological factors such as caries, trauma, infection, inflammation, or extraction, tooth eruption, nutritional deficit disorders, and Human papilloma virus (HPV)[5,6,7] as well as ameloblastin deficiency[8] have been considered in recent articles but these factors have been controversial and not conclusive[9,10,11,12,13]. According to World Health Organization (WHO) classification[14,15], ameloblastomas are divided into 4 subtypes: solid/multicystic ameloblastoma (SMA), unicystic ameloblastoma (UA), desmoplastic ameloblastoma (DA) and extraosseous (peripheral) ameloblastoma (EA). Two growth patterns including follicular pattern and plexiform pattern were recognized in ameloblastomas.

Patients with ameloblastomas occurred in 4 to 92 year-old with no significant difference in gender[16]. Ameloblastoma grows slowly and often results in swelling on face. The tumors enlarge their size with destraction of the cortical bone and the roots of teeth as well as with infiltration into the soft tissue. Delayed tooth eruption, tooth displacement, ulceration, pain and

paresthesia of lower lip were occasionally found in clinical findings from the patients with ameloblastomas[16]. The ratio between maxillary and mandibular ameloblastomas were reported as 1:5.8[16]. Unicystic ameloblastoma was often seen in young patients (the mean of age was 26.3 years) whereas solid/multicystic one in patients with higher age (the mean of age was 41.4 years)[16].

Nakamura et al.[17] advocated for conservative treatment but conservative treatment leads high recurrence rate. Chapelle et al.[18] recommended radical treatment for solid/multicystic ameloblastoma and unicystic ameloblastoma with aggressively histopathological features such as mural/intra mural ameloblastomas. The patients, then, should be followed up for at least 10 years.

The p53 protein, tumor suppressor protein, is the cellular gatekeeper against the formation of tumors. In normal cells, wild-type p53 protein is maintained at a low concentration due to its short half-life (about 20 minutes) and can inhibit cell proliferation. The loss of its function due to the mutation or alteration of the structure of p53 gene is also associated with increase its concentration as its extended half-life[19,20]. In addition, the expression of p53 in benign ameloblastoma was significantly higher than that in normal tissue[21]. On the other hand, pRB, the product of the retinoblastoma tumor suppressor gene, plays an important role in regulation of not only cell proliferation but also apotosis[22]. As we have known that Ki67 protein is well known as a marker of

cell proliferation expressed during all active phases of cell cycle except G0. The immuno-reactivity of Ki67 in previous study has showed similar distribution to that for Retinoblastoma protein (pRB) in ameloblastomas[23]. Moreover, fibroblast growth factor (FGF) signaling pathway was implicated as a key driver of tumor progression and growth including angiogenesis, proliferation, migration and differentiation, and cell survival as well as angiogenesis[24,25,26,27,28]. In particular, FGF-1 and FGF-2 have been shown as angiogenesis[25,26,27,28] and can directly affect tumor angiogenesis by promoting the cellular proliferation of endothelial cells[26,29]. FGF-1 and FGF-2 has been shown to contribute to the growth and development of ameloblastomas[30]. Furthermore, heparin-binding protein 17/fibroblast growth factor-binding protein-1 (HBp17/FGFBP-1) is secreted protein which was first purified from culture medium conditioned by human epidermoid carcinoma cell line A431-AJC[31]. HBp17/FGFBP-1 can bind FGF-1 and FGF-2 in a reversible, noncovalent manner and release them from the extracellular matrix[31,32]. Several studies showed that HBp17/FGFBP-1 might enhance FGF effect leading angiogenesis, tumor proliferation, migration and differentiation[24,25,26,27,33,34].

There have been several studies which evaluate the expression of Ki67, p53, pRB, FGF-1, FGF-2 as well as microvessel density (MVD) in ameloblastoma since then, but little is known about the correlation of pRB with Ki67, p53 as well as the expression and the correlations of HBp17/FGFBP-1 and FGF-1, FGF-2, MVD in ameloblastomas and the etiological features as well.

Aim of study

To elucidate the molecular etiological roles and the correlations of pRB, p53, Ki67, HBp17/FGFBP-1, FGF-1, FGF-2, and CD34 in ameloblastomas, the expression of these factors was studied immunohistochemically and examined the correlation between the each protein expression statistically.

2. Materials & Methods

Tissue samples of ameloblastomas from both of National Hospital of Odonto-Stomatology at Ho Chi Minh city, Viet Nam and Hiroshima University Hospital, Hiroshima, Japan were collected and studied reactivity for HBp17/FGFBp-1, FGF-1, FGF-2, CD34, p53, pRB and Ki67 markers immunohistochemically. All tissue samples were fixed in 10% neutral buffered formalin (Wako Pure Chemical Industries, Ltd. Osaka; Vinachem, Viet Nam) and embedded in paraffin (Histprep 580, Wako).The sections were prepared at 4 µm thickness for immunohistochemical procedures by using antibodies of HBp17/FGFBP-1, FGF1, FGF2, CD34, p53, pRB and Ki67 as shown in Table 1. This study has been approved by the Ethics Committee in Hiroshima University.

Heat-induced epitope retrieval method

For antigen retrieval, deparaffinized sections were pre-treated using heat-induced epitope retrieval method before blocking endogenous peroxidase activity.

For Ki67, pRB and CD34 antigen retrieval, Dako Target retrieval solution (pH 6.0, Dako, Glostrup, Denmark) was used. For p53 antigen retrieval, Tris-EDTA retrieval buffer (10mM Tris Base, 1mM EDTA solution, pH 9.0) was used.

Deparaffinized sections in the retrieval solution were pre-treated in microwave until the retrieval solution comes to boil (about 6 minutes), then further incubate them in the boiling water for 30-60 minutes.

Immunohistochemistry

After blocking endogenous peroxidase activity using 3% hydrogen peroxide (H_2O_2) (Wako) diluted in methanol (Nacalai tesque, Kyoto) for 30 minutes at room temperature, the sections were incubated with 10% normal goat serum (Histofine, Nichirei Bioscience Inc., Tokyo) at room temperature for 10 minutes to prevent non-specific binding and then incubated overnight with primary antibodies as shown in Table 1, at 4^0C.

For double antigens (CD34 and Ki67 (or p53)) staining, the sections were incubated with first primary antibody of CD34 for 30 minutes at room temperature, then further incubated overnight with second primary antibody of Ki67 or p53 followed by incubation with the corresponding secondary antibodies as shown in Table 1 for 30 minutes at room temperature.

As negative controls, sections were probed with diluted antibody solution except for primary antibody, or negative control mouse IgG1 (code X0931, Dako). As positive controls, sections from squamous cell carcinoma tissues and normal oral tissues were used.

The immuno-reactivities were visualized by using Dako Envision+System-HRP kits (Dako). The sections were then counterstained with Mayer's Hemalum solution (Merck, Germany) and permanently mounted.

Evaluations

For evaluating the expression of these factors, the sections were scanned at low magnification for localization of positive cells areas and microvessels' hot spots. Several fields, randomly selected were transferred to digital photomicrographs using Leica system (Leica DFC camera, type Leica DC500, Leica microsystems Imaging solution Ltd.,Tokyo). An ImageJ software (ImageJ 1.42q, public domain software, available at http://rsb.info.nih.gov/ij/index.html developed by Wayne Rasband) was used to count the number of positive tumor cells, number of negative tumor cells, tumor optical density (TOD), stroma optical density (SOD), optical density of the absolute white color, number of microvessels, the area of microvessels as well as the area of stroma.

Evaluation of HBp17/FGFBP-1, FGF1, FGF2, p53, pRB and Ki67 expression

Several randomized fields (x400) were selected and transfered to digital photomicrographs of 1300x1034 pixels using Leica system. By using the criteria and the results of previous studies[30,35,36,37], only cytoplasmic immuno-reactivity for HBp17/FGFBP-1, FGF1, FGF2 and only nuclear reactivity of pRB above any cytoplasmic background as well as nulcear immunoreactivity for p53, Ki67 were considered and evaluated as positive staining. At least 1000 tumor cells were counted. For evaluation of HBp17/FGFBP-1, FGF1, FGF2, p53, pRB and Ki67 expression, the labeling index (LI) and the digital expression index (dEI) were used according to the following formulas:

Labeling index (LI):

$$LI = \frac{\text{Number of positive cells}}{\text{Total cells}} 100(\%)$$

Digital immunostaining intensity (dISI): to count the digital immunostaining intensity (dISI), the same photomicrographs used for the counting LI were studied. 10 randomly selected regions from different positive tumor cells' areas and stroma's areas were indicated by using a "10-pixel-brush selections"- a tool of ImageJ software. The tumor optical density (TOD) and the stroma optical density (SOD) were then calculated. Optical density is the average of red, green and blue color component (RGB), expressed in optical units per pixel (ou/pixel). The absolute white color composed by the totality of red, green, and blue that corresponds to the maximum optical density (255 ou/pixel); and the absolute black color is the absence of these colors (0 ou/pixel). The formula below was used to calculate the digital immunostaining intensity (dISI). The value of each case was made up an increasing scale by equalizing with the stroma optical density and proportional to the optical density of the absolute white color[38].

Digital immunostaining intensity (dISI):

$$dISI = \frac{255.(SOD - TOD)}{SOD} \text{ (ou/pixel)}$$

The digital expression index (dEI) is obtained by multiplying the LI and the digital immunostaining intensity (dISI).

Digital expression index (dEI):

$$dEI = \frac{LI.dISI}{100} \quad (ou/pixel)$$

Evaluation of CD34 expression for tumor microvessels analysis:

The endothelial cells in microvessels were stained strongly and exclusively with CD34 marker. After scanning several areas within 500 µm around the tumor islands or in the center of tumor islands or within 500 µm under basement membrane at 200-fold magnification[(39)], 5 highest microvessels areas (hot spots) were selected. These selected areas (440x350µm) were transfered to digital photomicrographs of 1300x1034 pixels with Leica system. Based on the criteria of Weidner et al.[(40)], any positive endothelial cell or endothelial-cell cluster that was clearly separate from adjacent microvessels, tumor cells, and other connective-tissue elements was regarded as a distinct microvessel. Red cells were not required, nor were the presence of vessel lumens. By using ImageJ software, the area of CD34-positive microvessels and the area of stroma in each selected field as well as the number of microvessels were counted. Microvessel density (MVD), which defined as number of microvessels per mm^2 stroma and the percentage of total microvessel area size in stroma (pTS) (%) were assessed according to the following formulas:

Microvessel density (MVD):

$$MVD = \frac{\text{Total number microvessels}}{1\ mm^2\ \text{stroma}}$$

Percentage of total microvessel area size in stroma (pTS):

$$pTS = \frac{\text{Total microvessels area size}}{\text{Stroma area size}}\ 100\ (\%)$$

Evaluation of tumor size:

The estimated tumor volume (eV) has been calculated based on orthopanthomogram. By using a millimeter (mm) ruler, the height (H, mm) and the length (L, mm) of ameloblastoma were measured on orthopanthomogram. The eV was calculated according to the following formula:

Estimated tumor volume (eV):

$$eV = \frac{H.H.L}{2}\ (mm^3)$$

Statistical analysis

The Spearman's rank correlation test was used to examine statistical correlations of each protein expression of HBp17/FGFBP-1, FGF-1, FGF-2, p53, pRB, Ki67 and MVD, pTS as well as the estimated tumor volume. Scatter plots with the correlation lines were used to show the significant correlations

between them. The significance is indicated by the p value. Asterisk * indicates significant correlation ($p<0.05$). Wilcoxon signed-rank test (Mann-Whitney U test) was also used to examine the differences of HBp17/FGFBP-1 dEI, FGF1 dEI, FGF2 dEI, p53 dEI, pRB dEI, Ki67 dEI, MVD and pTS between the solid/multicystic ameloblastomas (SMA) and unicystic ameloblastomas (UA). Kruskal-Wallis test was used to examine the significant difference in the expression of these factors among groups of age.

3. Results

Clinical and histological characteristics of ameloblastomas

Twenty nine cases of benign ameloblastoma from 15 women and 14 men were studied (Table 2). The follicular patterns and the plexiform patterns (Figure 1A, 1B) in solid/multicystic ameloblastomas were occasionally seen in the same sections of the samples (data not shown). Twenty four ameloblastomas were found in the posterior mandible and 5 cases in the anterior mandible. Radical treatment such as mandibular resection was performed for 16 cases of benign ameloblastomas, all from National Hospital of Odonto-Stomatology at Ho Chi Minh city and conservative treatment such as marsupialization or enucleation was performed for 13 cases from Hiroshima University Hospital. Eight cases were recured after conservative treatment.

No case of ameloblastoma in maxillary was collected. Two cases of ameloblastic carcinoma also collected and the malignant cases were also included in this study (Table 2).

Expression of HBp17/FGFBP-1, FGF-1, FGF-2, CD34, p53, pRB and Ki67 in ameloblastomas

Immunohistochemical reactivity for HBp17/FGFBP-1 in ameloblastomas was mainly observed in the membrane and cytoplasm of the peripheral/basal cells, in the squamous cells as well as in the stellate reticulum-like cells (Figure 2A, 2B, 2C, 2D). The strongest staining intensity was seen in the squamous cells and in the peripheral/basal cells.

FGF1-positive staining was mainly observed in the squamous cells and in the cytoplasm of the peripheral/basal cells with the expansion into the stellate reticulum-like cell areas (Figure 3A, 3B, 3C, 3D). Squamous cells and peripheral/basal cells exhibited strong staining intensity.

The expression of FGF-2 was mainly detected in the membrane and in the cytoplasm of the peripheral/basal cells as well as in the squamous cells with spreading to the stellate reticulum-like cells (Figure 4A, 4B, 4C, 4D). The stellate reticulum-like cells areas showed weaker staining intensity compare to that in the squamous cells and in the peripheral/basal cells areas.

HBp17/FGFBP-1, FGF-1, and FGF-2- positive staining was occasionally seen in the nuclei of tumor cells.

Tumor microvessels with endothelial cells expressing strong staining intensity of CD34 showed slightly irregular shaped, tortuous and dilated form in the stroma (Figure 5A, 5B, 5C, 5D). Follicular patterns (Figure 5A, 5C) showed many small microvessels with slightly irregular shape, whereas microvessels in plexiform patterns were scattered with dilated shape (Figure 5B, 5D).

The immunohistochemical reactivity for p53 was detected in the nuclei of peripheral/basal cells with spreading to the stellate reticulum-like cells (Figure 6A, 6B, 6C, 6D). The p53-positive cells in the reticulum-like cell area showed lower intensity than that in the peripheral/basal cell area.

Immunohistochemical reactivity for pRB in ameloblastomas was mainly recognized in the nuclei of the tumor cells (Figure 7A, 7B, 7C, 7D). The pRB-

positive cells in the peripheral/basal areas exhibited stronger staining intensity than those in the stellate reticulum-like areas.

The expression of Ki67 protein in ameloblastomas was observed in nuclei of tumor cells with strong immunostaining intensity (Figure 8A, 8B, 8C, 8D). A few scattered Ki67-positive cells were observed in the peripheral/basal cells and occasionally seen in the stellate reticulum-like cells. There is no significant difference in an intensity of Ki67-positive cells between the stellate reticulum-like cell area and the peripheral/basal cell area.

Double Ki67-CD34 antigens staining

The higher expression of Ki67 in tumor cells was associated with an increase in microvessels around tumors islands (Figure 9A, 9B, 9C, 9D). Tumor islands with high expression of Ki67 accompanied with many small microvessels with irregular shape in tumor of follicular patterns (Figure 9A, 9B) whereas tumor islands with high expression of Ki67 have very few microvessels with dilated shape in plexiform patterns (Figure 9C, 9D).

Correlation between p53, pRB and Ki67

It has been found that p53 dEI positively correlated with Ki67 dEI (p=0.02) (Figure 10B, Table 3B) whereas no correlation between p53 LI and Ki67 LI (p=0.094) has been observed (Figure 10A, Table 3A).

The positive correlations between pRB and p53, Ki67 were revealed in the scatter plots (Figure 11). By using the Spearman rank correlation's test, the LI of

pRB showed significantly positive correlation with that of p53 (p<0.001) and that of Ki67 (p=0.003) (Figure 11A, Table 3A). In addition, the dEI of pRB showed significantly positive correlation with that of p53 (p<0.001) and that of Ki67 (p=0.009) (Figure 11B, Table 3B).

Correlation between Ki67 and MVD and pTS

It has been found that pTS correlated well with Ki67 LI (p=0.001) and Ki67 dEI (p=0.002) (Figure 12B) but MVD did not correlated with Ki67 LI (p=0.157) and Ki67 dEI (p=0.221) (Figure 12A).

Correlation between tumor angiogenesis, tumor microvessels and tumor proliferation

The dEI of HBp17/FGFBP-1 has significantly positive correlation with FGF-1 dEI (p<0.001), FGF-2 dEI (p<0.001), MVD (p<0.001), and pTS (p<0.001) (Figure 13A, 13B; Table 5). The significantly positive correlation between pTS with FGF-1 dEI (p<0.001), and FGF-2 dEI (p<0.001) as well as MVD with FGF-1 dEI (p<0.001), and FGF-2 dEI (p<0.001) are also found in this study (Table 5).

The dEI of Ki67 also correlated with HBp17/FGFBP-1 dEI (0.002), FGF-1 dEI (p=0.004), and FGF-2 dEI (p=0.038) (Figure 14, Table 5).

The role of p53 in tumor angiogenesis in ameloblastomas

The positive correlation of p53 and HBp17/FGFBP-1, FGF-1, FGF-2, MVD and pTS was obtained (p<0.001) on the scatter plots analysis (Figure 15A, 15B).

Correlation of the expression of several factors with tumor size (estimated tumor volume)

An eV calculated from orthopanthomogram significantly correlated with HBp17/FGFBP-1 dEI (p=0.024) and pRB dEI (p=0.008) (Figure 16). There is no significant correlation between eV and the expression of other factors (p>0.05).

Correlation of the expression of several factors with age

The age of patients with ameloblastmas were divided into 3 groups, group 1 with patients younger than 20 years, group 2: patients from 20-40 years and groups 3 with patients older than 40 years. It has been found that pRB dEI, and pRB LI showed significant difference amongst three groups of age (Table 6).

Relationship between the expression of several factors and the gender and location of tumors

There was no significant gender and location difference in the expression of these factors.

Difference in the expression of the various factors between SMA and UA

The p53 LI in SMA was significantly higher than that in UA (p=0.046) whereas the dISI of p53 in UA was significantly higher than that in SMA (p=0.036). There is no difference in dEI of p53 between SMA and UA (p=0.178) (Table 7).

Moreover, there is no difference in the expression of HBp17/FGFBP-1, FGF-1, FGF-2, CD34, pRB and Ki67 between SMA and UA (Table 7).

Other results

The expression of the factors in ameloblastic carcinoma was higher than that in benign ameloblastomas, but due to small sample size, the statistical comparison of the expression of these factors between malignant and benign ameloblastomas could not be performed (Table 8).

4. Discussion

The p53 protein, tumor suppressor protein, is the cellular gatekeeper against the formation of tumors due to its ability to protect the genome by responding to genotoxic stress, such as DNA damage and other stress signals. In normal cells, wild-type p53 is maintained at a low concentration due to its short half-life (about 20 minutes). The loss of its function either due to mutation or alteration of the structure of p53 gene is also associated with increased its concentration as its extended half-life[19,20]. Kumamoto et al.[21] showed that the expression of p53 in ameloblastomas was significantly higher than that in normal tissues suggesting the abnormal p53 in ameloblastomas might be the results of the loss of its function leading to the formation and the development of ameloblastomas. Although several studies demonstrated existence of mutation of p53 in ameloblastomas, there has been speculated that the mutation might play a minor role in neoplastic changes of ameloblastomas[21,41,42,43]. In this study, an immunohistochemical reactivity for p53 was seen in the nuclei of peripheral/basal cells with spreading of p53-positive cells to the stellate reticulum-like cells. The p53-positive staining intensity in the peripheral areas exhibited stronger than that in the stellate reticulum-like cells areas.

It has been reported that the expression of Ki67 protein reflecting to cellular proliferation ability expressed maximally during S-phase and rapidly degraded after mitosis. Thus it has been known that Ki67 is an useful marker to predict for tumor development[44,45]. In ameloblastomas, a few scattered Ki67-

positive cells were observed only limited area in the peripheral/basal areas, at where the proliferating tumor cells exist in ameloblastoma[46,47,48] although some positive cells were detected in the stellate reticulum-like cells areas. The staining intensity of Ki67-positive cells in the stellate reticulum-like cell areas is similar to that of the peripheral/basal cell areas.

Normally, p53 can inhibit cell proliferation but loss of its function results in increased proliferation. Several studies demonstrated the correlation between p53 and Ki67 in tumors[39,49,50]. Slootweg[51] demonstrated that increased p53 staining intensity rather than increased the number of p53-positive cells was well related to proliferation in odontogenic epithelium. In my study, the significantly positive correlation between p53 dEI and Ki67 dEI was found whereas the correlation between p53 LI and Ki67 LI was not observed, suggesting dEI is more useful indicator compare to LI in evaluating the immunohistochemical expression.

Besides, tumor growth is the result of the interaction between cell proliferation and cell death in which the balance between proliferation and apoptosis plays an important role in tumor growth[22,33,45,52,53,54,55]. In normal tissue, the balance between proliferation and apoptosis is maintained[54,56] whereas in ameloblastomas, the positive correlation between p53 and Ki67 showed the loss of this balance. In addition, pRB, the product of the retinoblastoma tumor suppressor gene, plays an important role in regulation of not only cell proliferation but also apotosis[54,57,58]. The pRB can repress

transcription by at least two different mechanisms: bind E2Fs and block their ability to activate transcription; pRB-E2F repressor complex that forms at promoters can actively repress transcription[22]. Thus, pRB can inhibit cell proliferation. Although several studies showed the role of HPV in inhibition of pRB[59], there is no evidence whether HPV works as the etiologically important role in ameloblastomas[10,13]. Recent study suggested that the presence of HPV-DNA in ameloblastomas could be explained by secondary surgically acquired contamination from the surface mucosal epithelium than a true integration of HPV-DNA in human genome[9]. On the other hand, pRB can regulate the apoptotic function as an upstream regulator of p53[60] through binding to MDM2, thus it might protect p53 from MDM2-targeted degradation by occupying a site on MDM2[61]. However, pRB can regulate the cell proliferation and apoptosis through the phosphorylation cycle, in which hyperphosphorylated pRB repeals the interaction with E2F allowing free E2Fs to control the expression of several genes that are involved in the cell proliferation and apoptosis[22]. Thus, pRB plays an important role in the regulation of the balance between proliferation and apoptosis.

In this study, the immunohistochemical reactivity for pRB is mainly observed in the nuclei and occasionally seen in the cytoplasm. The pRB-positive cells in the peripheral/basal areas exhibited stronger staining intensities than those in the stellate reticulum-like areas. In this study, the positive correlation between the expression of pRB and the expression Ki67 has been found. This

result is in good agreement with the previous reports that the expression of pRB correlated with cell proliferation of neoplastic odontgenic epithelial cells [22,23,54,62,63,64,65]. The positive correlation between pRB and Ki67 in ameloblastoma suggested the loss of precise function of pRB in inhibition of the growth leading proliferation. While pRB can regulate the apoptotic function as an upstream regulator of p53[60], p53 also has ability to induce expression of p21, which in turn can shut down the cyclin-CDK complexes leading G1/S arrest and therefore maintains pRB in the growth suppression state[66]. The positive correlation between the expression of pRB and p53 obtained in this study strongly suggests the close relationship between pRB and p53 in ameloblastomas. As pRB plays an important role in the balance between the proliferation and apoptosis, the loss of this balance due to the loss of precise function of either pRB or p53 might be involved in the etiology of ameloblastomas.

Angiogenesis has been well known to play an important role in development, and progression of tumors[67.68]. It has been well known that tumors are not able to enlarge their size bigger than 2.5 mm in diameter without recruiting new microvessels[28,68,69]. A CD34 is a monomeric glycoprotein that shows strong and exclusive expression in the endothelial cells. Its expression is often used to evaluate microvessel density (MVD) in tumors[70,71,72]. According to Weidner et al.[40], any positive endothelial cell or endothelial-cell cluster that was clearly separate from adjacent microvessels,

tumor cells, and other connective-tissue elements was regarded as a distinct microvessel. Red cells were not required, nor were the presence of microvessel lumens. Single cell sprouts as well as large size of microvessels were included in the counts. A cross-sectional area size of microvessel is not mentioned whether its size is small or large. Even more than once of distinct clusters given by one large size of microvessel by the transected plane, these distinct clusters should be regarded as separate microvessels and they were included in the counts leading high MVD. Tumor with high MVD means tumor has a lot of microvessels in a field but the amount of blood supply could depend not only on the number of microvessels but also on the volume of microvessels. The amount of blood supply of a small number of large volumes of microvessels could be similar to that of a higher number of small volumes of microvessels around tumor islands. This suggests that the larger the dilatation of tumor microvessels, the more increased the surface area of microvessels and the higher the blood supply[73]. High MVD and pTS have been considered as the result of increased angiogenesis[74]. In this study, pTS but not MVD correlated well with Ki67 suggesting increase in the percentage of microvessels area size in stroma rather than increase in the number of microvessels correlated with tumor proliferation. The percentage of microvessels area size in stroma might play an important indicator in the growth of ameloblastomas.

A secreted protein, Heparin-binding protein 17/fibroblast growth factor-binding protein-1 (HBp17/FGFBP-1), was first purified from culture medium

conditioned by human epidermoid carcinoma cell line A431-AJC[31]. It has been well known that HBp17/FGFBP-1 plays an important role in tumor angiogenesis as well as in tumor growth and progression[75,76]. HBp17/FGFBP-1 can bind FGF-1 and FGF-2 in a reversible, noncovalent manner and release them from the extracellular matrix[31,32]. In addition, several studies showed HBp17/FGFBP-1 enhanced the effects of FGFs leading angiogenesis, tumor proliferation, migration and differentiation[24,25,26,27,33,34]. The expression of HBp17/FGFBP-1 was overexpressed in tumor cells compare to normal epithelial cells[29,35]. In ameloblastomas, expression of HBp17/FGFBP-1 was found in the membrane and cytoplasm of peripheral/basal cells, in the cytoplasm of the stellate reticulum-like cells, as well as in the squamous cells although the strongest staining intensities were seen in the squamous cells and the peripheral/basal cells. The nuclei of tumor cells were occasionally detected positive reactivity for HBp17/FGFBP-1. These suggest that HBp17/FGFBP-1 might be produced and secreted by ameloblastoma cells and play roles in regulation of tumor angiogenesis and stimulation of tumor progression.

Fibroblast growth factor (FGF) signaling pathway is well known as a key driver of tumor progression and growth including wound repair, cell proliferation, migration, differentiation, and cell survival as well as angiogenesis[24,25,26,27]. Aberrations in this signaling pathway may drive tumorigenesis[25]. FGFs such as FGF-1 and FGF-2 have been shown as angiogenic factors[25,26,27,70] and can directly affect tumor angiogenesis by

promoting the cellular proliferation of endothelial cells[26,29]. Besides, several studies showed FGF-1 and FGF-2 had an important role for new blood vessel growth[67,77] and FGF-2 was a powerful inducer of angiogenesis which was twice as poweful as VEGF[33]. In previous study, it has been shown that both FGF-1 and FGF-2 contribute to the growth and the development of ameloblastomas by culturing ameloblastoma-derived tumor cells[30]. In this study, important role of FGF-1 and FGF-2 in tumor angiogenesis has been revealed by the significantly positive correlation of FGF-1 dEI and FGF-2 dEI with MVD and pTS.

Moreover, HBp17/FGFBP-1 dEI has had significant correlation with FGF-1, FGF-2 and MVD, pTS in this study. The results were in agreement with previous studies by Aigner A. et al.[78]. They showed that HBp17/FGFBP-1 can serve as an angiogenic switch molecule of which down-regulation showed inhibition of angiogenesis. Moreover, Ray R. et al.[79] reported that up-regulation of HBp17/FGFBP-1 was significantly correlated with increased MVD. These results strongly suggest the important role of HBp17/FGFBp-1 in the growth and progression of amleoblastomas. Taken together, HBp17/FGFBP-1 together with FGF-1, FGF-2 might play important roles in the progression of tumor growth through stimulating tumor angiogenesis and growth in ameloblastomas.

It has been demonstrated that p53 protein has roles in tumor growth suppressor and in apoptosis including cell cycle arrest, DNA repair, programmed cell death as well as the role in inhibition of tumor angiogenesis[19,20,39,80,81]. In normal cells, p53 protein can inhibit angiogenesis by

at least three mechanisms: 1) interfering with central regulators of hypoxia that mediate angiogenesis; 2) inhibiting production of proangiogeneic factors; 3) directly increasing the production of endogenous angiogenesis inhibitors[20]. The combinatory effects allow p53 to inhibit angiogenesis. Loss of its function can reverse these effects, as consequence, p53 can induce angiogenesis. Bergers et al.[80] demonstrated that wild-type p53 inhibits vascular endothelial growth factor (VEGF) transcription and prevent progression of tumors and their metastases whereas cells with p53 defects have up-regulated the expression of VEGF leading tumor angiogenesis. In this study, p53 expression is significantly correlated with that of HBp17/FGFBP-1, FGF-1, FGF-2, MVD, pTS, suggesting the function of p53 in tumor angiogensis in ameloblastomas.The expression of pRB might be influenced by tumor size and age of the patients in ameloblastomas. Moreover, tumor size might also influence the expression of HBp17/FGFBP-1. The process of tumor growth and invasion in SMA might be same as that in UA.

5. Conclusions

1. The dEI is more useful indicator than LI in evaluating the immunohistochemical expression.
2. The increase in percentage of microvessel area size in stroma rather than increase in number of microvessels correlated with tumor growth and progression in ameloblastomas.
3. The HBp17/FGFBP-1 together with FGF-1, FGF-2 play an important role in the progression of the tumor growth through stimulating tumor growth and angiogenesis in ameloblastomas.
4. The p53 plays an important role in inducing tumor angiogenesis in ameloblastomas.
5. The loss of the balance between proliferation and apoptosis due to the loss of precise function of either p53 or pRB might be involved in the molecular etiology of ameloblastomas.
6. The expression of pRB might be influenced by tumor size and age of the patients in ameloblastomas. Moreover, tumor size might also influence the expression of HBp17/FGFBP-1.
7. The process of tumor growth and invasion in SMA might be same as that in UA.

Conclusion: The HBp17/FGFBP-1, FGF-1, FGF-2, CD34, p53, pRB and Ki67 play important roles in the development and progression of ameloblastomas.

References

1. Cusack JW. Report of the amputation of portions of the lower jaw. Dublin Hosp Rec 1827; **4**: 1-38.

2. Broca PP. Researches sur in nouveau groupe de tumeurs designées sous le nom d'odontomes. Gaz Hebd Sci Méd 1868;**5**;70-84.

3. Malassez L. Sur le role des debris épitheliaux paradentaires. Arch Physiol Norm Pathol 1885;**5**:309-340 and 6:379-449.

4. Ivey RH, Churchill HR. The need of a standardized surgical and pathological classification of tumors and anomalies of dental origin. Am Assoc Dent Sch Trans 1930;**7**: 240–245.

5. Kahn MA. Ameloblastoma in young persons: a clinicopathologic analysis and etiologic investigation. Oral Surg Oral Med Oral Pathol. 1989 Jun ;**67** (6):706-15.

6. Mokhtari-Azad T, Moradi A , Khodayari-Nemin A , Keikhaee MR , Sargolzaei S, Shahrokhi M. Detection of Human Papillomavirus DNA in Intraosseus Ameloblastoma. International Journal of Virology 2006; **2**: 1-6.

7. Namin AK, Azad TM, Eslami B, Sarkarat f, Shahrokhi M, Kashanian F. A study of the relationship between ameloblastom and human papilloma virus. J Oral maxillofac Surg 2003; **61**:467-470.

8. Fukumoto S, Kiba T, Hall B, Iehara N, Nakamura T, Longenecker G, Krebsbach PH, Nanci A, Kulkarni AB, Yamada Y. Ameloblastin is a cell adhesion molecule required for maintaining the differentiation state of ameloblasts. J Cell Biol. 2004 Dec 6;**167**(5):973-83.

9. Correnti M, Rossi M, Avila M, Perrone M, Rivera H. Human papilloma virus in ameloblastoma. Oral Surg Oral Med Oral Pathol Oral Radiol Endod 2010; **110**:e20-e24.

10. Migaldi M, Pecorari M, Rossi R, Maiorana A, Bettelli S, Tamassia MG, Gaetani CD, Leocata , Portolani M. Does HPV play a role in the etiopathogenesis of ameloblastom? An immunohistochemical, in situ hybridization and polymerase chain reaction study of 18 cases using laser capture microdissection. Modern Pathology 2005; **18**: 283-289.

11. Perdigão PF, Gomez RS, Pimenta FJ, De Marco L. Ameloblastin gene (AMBN) mutations associated with epithelial odontogenic tumors. Oral Oncol. 2004 Sep;**40**(8):841-6.

12. Perdigão PF, Carvalho VM, DE Marco L, Gomez RS. Mutation of ameloblastin gene in calcifying epithelial odontogenic tumor. Anticancer Res. 2009 Aug;**29**(8):3065-7.

13. Sand L, Jalouli J, Larsson PA, Magnusson B, Hirsch JM. Presence of human papilloma viruses in intraosseous ameloblastom. J Oral Maxillofac surg 2000; **58**: 1129-1134.

14. Kramer IRH, Pindborg JJ, Shear M. WHO Histological Typing of Odontogenic Tumours. Springer-Verlag, Berlin, 1992. p. 11-27.

15. Gardner DG, Heikinheimo K, Shear M, Philipsen HP, Coleman H. WHO Classification of Tumours. Pathology and genetics of head and neck tumours: Odontogenic tumours. IARC Press: Lyon, 2005. p. 296-300.

16. Prætorius F. Surgical Pathology of Head and Neck 3rd Edition. Chapter 19: Odontogenic tumors. Informa Healthcare 2009. P.1201-1338.

17. Nakamura N, Higuchi Y, Mitsuyasu T, Sandra F, Ohishi M. Comparison of long-term results between different approaches to ameloblastoma. Oral Surg Oral Med Oral Pathol Oral Radiol Endod. 2002 Jan;**93**(1):13-20.

18. Chapelle KA, Stoelinga PJ, de Wilde PC, Brouns JJ, Voorsmit RA. Rational approach to diagnosis and treatment of ameloblastomas and odontogenic keratocysts. Br J Oral Maxillofac Surg. 2004 Oct;**42**(5):381-90.

19. Levine AJ. Review: p53, the cellular gatekeeper for growth and division. Cell Press 1997; **88**: 323-331.

20. Teodoro JG., Evans SK, Green MR. Review: Inhibition of tumor angiogenesis by p53: a new role for the guardian of the genome. J Mol Med (Berl) 2007 Nov;**85**(11):1175-1186.

21. Kumamoto H, Izutsu T, Ohki K, Takahashi N, Ooya K. p53 gene status and expression of p53, MDM2, and p14ARF proteins in ameloblastoma. J Oral Pathol Med 2004 May;**33**(5):292-299.

22. Weinberg RA. The biology of cancer. Chapter 8: pRB and control of the cell cycle clock. Galand Science, Taylor & Francis Group:LLC, 2007; p. 255-306.

23. Kumamoto H, Ooya K, Immunohistochemical detection of retinoblastoma protein and E2 promoter-binding factor-1 in ameloblastoma. J Oral Pathol Med 2006 Mar;**35**(3):183-9.

24. Beenken A. Mohammadi M. The FGF family:biology, pathology and therapy. Nat Rev Drug Disco 2009; 8: 235-253.

25. Daniele G, Corral J, Molife LR, de Bono JS. FGF receptor inhibitors: Role in Cancer Therapy. Curr Oncol Rep. 2012 Apr;**14**(2):111-119.

26. Lieu C, Heymach J, Overman M, Tran H, Kopetz S. Beyond VRGF: inhibition of the fibroblast growth factor pathway and antiangiogenesis. Clin Cancer Res. 2011 Oct 1;**17**(19):6130-6139.

27. Powers CJ, McLeskey SW, Wellstein A. Fibroblast growth factors, their receptors and signaling. Endocr Relat Cancer. 2000 Sep;**7**(3):165-197.

28. Folkman J, Shing Y. Angiogenesis. J. Biol. Chem. 1992;**267**: 10931-10934.

29. Okamoto T, Tanaka Y, Kan M, Sakamoto A, Takada K, Sato JD. Expression of fibroblast growth factor binding protein HBp17 in normal and tumor cells. In Vitro Cell Dev Biol Anim. 1996 Feb;**32**(2):69-71.

30. Myoken Y, Myoken Y, Okamoto T, Sato JD, Takada K. Immunohistochemical localization of fibroblast growth factor-1 (FGF-1) and FGF-2 in cultured human ameloblastoma epithelial cells and ameloblastoma tissues. J Oral Pathol Med. 1995 Oct;**24**(9):387-392.

31. Wu DQ, Kan MK, Sato GH, Okamoto T, Sato JD. Characterization and molecular cloning of a putative binding protein for heparin-binding growth factors. J Biol Chem. 1991 Sep 5;**266**(25):16778-16785.

32. Aigner A, Butscheid M, Kunkel P, Krause E, Lamszus K, Wellstein A, et al. An FGF-binding protein (FGF-BP) exerts its biological function by parallel

paracrine stimulation of tumor cell and endothelial cell proliferation through FGF-2 release. Int J Cancer. 2001 May 15;**92**(4):510-517.

33. Pepper MS, Ferrara N, Orci L, Montesano R. Potent synergism between vascular endothelial growth factor and basic fibroblast growth factor in the induction of angiogenesis in vitro. Biochem Biophys Res Commun. 1992 Dec 15;**189**(2):824-831.

34. Tassi E, McDonnell K, Gibby KA, Tilan JU, Kim SE, Kodack DP, et al. Impact of fibroblast growth factor-binding protein-1 expression on angiogenesis and wound healing. Am J Pathol. 2011 Nov;**179**(5):2220-2232.

35. Begum S, Zhang Y, Shintani T, Toratani S, Sato JD, Okamoto T. Immunohistochemical expression of heparin-binding protein 17/fibroblast growth factor-binding protein-1 (HBp17/FGFBP-1) as an angiogenic factor in head and neck tumorigenesis. Oncol Rep. 2007 Mar;**17**(3):591-596.

36. Pande P, Mathur M, Shukla NK, Ralhan R. pRB and p16 protein alteration in human oral tumorigenesis. Oral Oncol 1998 Sep;**34**(5):396-403.

37. Gadbail AR, Patil R, Chaudhary M. Co-expression of Ki-67 and p53 protein in ameloblastoma and keratocystic odontogenic tumor. Acta Odontol Scand. 2012 Dec;**70**(6):529-35.

38. de Matos LL, Stabenow E, Tavares MR, Ferraz AR, Capelozzi VL, Pinhal MAS. Immunohistochemistry quantification by a digital computer-assisted method compared to semiquantitative analysis. Clinics. 2006;**61**(5):417-424.

39. Gadbail AR, Hande A, Chaudhary M, Nikam A, Gawande M, Patil S, et al. Tumor angiogenesis in keratocystic odontogenic tumor assessed using CD-105 antigen. J Oral Pathol Med. 2011 Mar;**40**(3):263-269.

40. Weidner N, Semple JP, Welch WR, Folkman J. Tumor angiogenesis and metastasis – correlation in invasive breast carcinoma. N Engl J Med. 1991 Jan 3;**324**(1):1-8.

41. Al-Salihi KA, Li LY, Azilina A. p53 gene mutation and protein expression in ameloblastoma. Braz J Oral Sci 2006;**5**(17):1034-1040.

42. Gomez CC, Duarte AP, Diniz MG, Gomez RS. Review article: current concepts of ameloblastoma pathogenesis. J Oral Pathol Med 2010 Sep;**39**(8):585-591.

43. Salehinejad J, Zare-Mahmoodabadi R, Sahgafi S, Jafarian A, Ghazi N, Rajaei A, et al. Immunohistochemical detection of p53 and PCNA in ameloblastoma and adenomatoid odontogenic tumor. J Oral Sci 2011; **53**(2): 213-221.

44. Ross W, Hall PA. Ki67: from antibody to molecule to understanding?. Clin Mol Pathol 1995;**48** (3): M113-117.

45. Florescu A., Simionescu C., Ciurea R., Pitru A., p53, bcl-2 and ki67 immunoexpression in follicular solid ameloblastoma. Rom J Morphol Embryol 2012; **53**(1): 105-109.

46. Mitsuyasu T., Harada H., Higuchi Y., kimuraK., Nakamura N., Katsuki T. Immunohistochemical demonstration of bcl-2 protein in ameloblastoma. J Oral Pathol Med 1997; **26**:345-8.

47. Ong'uti M.N., Cruchley A.T.,Howells G.L., Williams D.M. Ki-67 antigen in ameloblastoma: correlation with clinical and histological parameters in 54 cases from Kenya. Int J. oral Maxillofac. Surg 1997;**26**: 376-379.

48. Sandra F., Mitsuyasu T., Nakamura N., Shiratsuchi Y., Ohishi M. immunohistochemical evaluation of PCNA and Ki-67 in ameloblastoma. Oral Oncol. 2001;**38**: 153-7.

49. Hosaka N., Ryu T., Cui W., Li Q., Nishida A., Miyake T., Takaki T., Inaba M., Ikehara S., Relationship of p53, Bcl-2, Ki67 index and E-cadherin expression in early invasive breast cancers with comedonecrosis as an accelerated apoptosis. J Clin Pathol 2006; **59**: 692-698.

50. Fourati A, El May MV, Ben Abdallah M, Gamoudi A, Mokni N, Goucha A, Boussen H, Ladgham A, El May A.; Prognostic evaluation of p53, heat shock protein 70, Ki67, and CD34 expression in cancer of the tongue in Tunisia; J Otolaryngol Head Neck Surg. 2009 Apr;**38**(2):191-6.

51. Slootweg PJ. P53 protein and Ki67 reactivity in epithelial odontogenic lesions. An immunohistochemical study. J Oral Pathol Med. 1995 Oct;**24**(9):393-7.

52. Babu NC, Dawra G, Sindura CS. Immunohistochemical evaluation of bcl-2 and cytokeratin 14 and cytokeratin 19 in ameloblastoma. International Journal of Contemporary Dentistry (IJCD) 2010; **1**(1): 36-39.

53. Gao Y., Yang L., Zhu X., Detection of the apoptosis suppressing oncoprotein bcl-2 in ameloblasstomas. Zhonghua Bing Li xue Za Zhi, 1995; **24**(2): 78-79.

54. Hickman ES., Moroni MC, Helin K. The role of p53 and pRB in apoptosis and cancer. Curr Op in Genet Dev. 2002 Feb;**12**(1):60-66.

55. Yamasaki L. Mini review: Balancing proliferation and apoptosis in vivo: the Goldilocks theory of E2F/DP action. Biochim Biophys Acta. 1999 Mar 25;**1423**(2):M9-15.

56. Bates S, Phillips AC, Clark PA, Stott F, Peters G, Ludwig RL, et al. p14ARF links the tumour suppressors RB and p53. Nature 1998 Sep 10; **395**:124-125

57. Müller H, Bracken AP, Vernell R, Moroni MC, Christians F, Grassilli E, et al. E2Fs regulate the expression of genes involved in differentiation, development, proliferation, and apoptosis. Genes Dev 2001 Feb 1;15(3):267-85.Nakamura N, Higuchi Y, Mitsuyasu T, Sandra F, Ohishi M. Comparison of long-term results between different approaches to ameloblastoma. Oral Surg Oral Med Oral Pathol Oral Radiol Endod. 2002 Jan;**93**(1):13-20.

58. Peeters CF, de Waal RM, Wobbes T, Westphal JR, Ruers TJ. Outgrowth of human liver metastases after resection of the primary colorectal tumor: A shift in the balance between apoptosis and proliferation. Int J Cancer. 2006 Sep 15;**119**(6):1249-1253.

59. Song S, Gulliver GA, Lambert PF. Human papillomavirus type 16 E6 and E7 oncogenes abrogate radiation-induced DNA damage responses in vivo through p53-dependent and p53-independent pathways. Proc Natl Acad Sci U S A. 1998 March 3; **95**(5): 2290–2295.

60. Xu HJ, Quinlan DC, Davidson AG, Hu SX, Summers CL, Benedict WF. Altered retinoblastoma protein expression and prognosis in early-stage non-small-cell lung carcinoma. J Natl Cancer Inst 1994 May 4;**86**(9):695-699.

61. Hofmann F, Martelli F, Livingston DM, Wang Z. The retinoblastoma gene product protects E2F-1 from degradation by the ubiquitin-proteosome pathway. Genes Dev 1996; 10: 2949–2959.

62. Cordon-Cardo C, Richon VM. Expression of the retinoblastoma protein is regulated in normal human tissues. Am J Pathol. 1994 March; **144**(3): 500–510.

63. Jares P, Campo E, Pinyol M, Bosch F, Miquel R, Fernandez PL, et al. Expression of retinoblastoma gene product (pRb) in mantle cell lymphomas. Correlation with cyclin D1 (PRAD1/CCND1) mRNA levels and proliferative activity. Am J Pathol. 1996 May;**148**(5):1591-600.

64. Martinez JC, Piris MA, Sánchez-Beato M, Villuendas R, Orradre JL, Algara P, et al. Retinoblastoma (Rb) gene product expression in lymphomas. Correlation with Ki-67 growth fraction. J Pathol. 1993 Apr;1**69**(4):405-12.

65. Seki S, Kawakita N, Yanai A, Kitada T, Sakai Y, Nakatani K, et al. Expression of the retinoblastoma gene product in human hepatocellular carcinoma. Hum Pathol. 1995 Apr;**26**(4):366-374.

66. Harrington EA, Bruce JL, Harlow E, Dyson N. pRb plays an essential role in cell cycle arrest induced by DNA damage. Proc Natl Acad Sci U S A. 1998 Sep 29;**95**(20):11945-11950.

67. Folkman J. Angiogenesis in cancer, vascular, rheumatoid and other disease. Nat Med. 1995 Jan;**1**(1):27-31.

68. Risau W. Mechanisms of angiogenesis. Nature. 1997 Apr 17;**386**(6626):671-674.

69. Folkman J. Angiogenesis in psoriasis: therapeutic implication. J Invest Dermatol. 1972 Jul;**59**(1):40-43.

70. Kademani D, Lewis JT, Lamb DH, Rallis DJ, Harrington JR. Angiogenesis and CD34 expression as a predictor of recurrence in oral squamous cell carcinoma. J Oral Maxillofac Surg. 2009 Sep;**67**(9):1800-1805.

71. Lanza F, Healy L, Sutherland DR. Structural and functional features of the CD34 antigen: an update. J Biol Regul Homeost Agents. 2001 Jan-Mar;**15**(1):1-13.

72. Vartanian RK, Weidner N. Correlation of intratumoral endothelial cell proliferation with microvessel density (tumor angiogenesis) and tumor cell proliferation in breast carcinoma. Am J Pathol. 1994 Jun;**144**(6):1188-1194.

73. Koizumi Y, Kauzman A, Okada H, Kuyama K, McComb RJ, Yamamoto H. Assessment of proliferative activity and angiogenesis in ameloblastoma: A comparison based on patient age. Int J Oral Med Sci 2004; **3**(1): 25-33.

74. Li C, Shintani S, Terakado N, Klosek SK, Ishikawa T, Nakashiro K, Hamakawa H. Microvessel density and growth factor, and platelet-derived endothelial growth factor in oral squamous cell carcinomas. Int J Oral Maxillofac Surg. 2005 Jul;**34**(5):559-565.

75. Czubayko F, Smith RV, Chung HC, Wellstein A. Tumor growth and angiogenesis induced by a secreted binding protein for fibroblast growth factors. J Biol Chem. 1994 Nov 11;**269**(45):28243-28248.

76. Tassi E, Henke RT, Bowden ET, Swift MR, Kodack DP, Kuo AH, et al. Expression of a fibroblast growth factor-binding protein during the development of adenocarcinoma of the pancreas and colon. Cancer Res. 2006 Jan 15;**66**(2):1191-1198.

77. Broadley KN, Aquino AM, Woodward SC, Buckley-Sturrock A, Sato Y, Rifkin DB, et al. Monospecific antibodies implicate basic fibroblast growth factor in normal wound repair. Lab Invest. 1989 Nov;**61**(5):571-575.

78. Aigner A, Renneberg H, Bojunga J, Apel J, Nelson PS, Czubayko F. Ribozyme-targeting of a secreted FGF-binding protein (FGF-BP) inhibits proliferation of prostate cancer cells in vitro and in vivo. Oncogene. 2002 Aug 22;**21**(37):5733-5742.

79. Ray R, Cabal MR, Moser AR, Waldman T, Zipper LM, Aigner A, Byers SW, Riegel AT and Wellstein A. Upregulation of fibroblast growth factor-binding protein, by beta-catenin during colon carcinogenesis. Cancer Res. 2003 Dec 1;**63**(23):8085-9.

80. Bergers G., Benjamin L.E.. Reviews: Tumorigenesis and the angiogenic switch. Nature reviews. Cancer 2003; **3**: 401-410.

81. Nikumthorn N., Yanatatsaneejit P., Rabalert J., Dhammawipark C., Mutirangura A., Association of p53 codon 72 polymorphism and ameloblastoma. Oral Disease 2012; **16**: 631-5.

Figure Legends

Figure Legends

Figure 1: Hematoxylin and Eosin staining. Follicular pattern (1A), Plexiform pattern (1B) (x200).

Figure 2: Immunohistochemical staining for HBp17/FGFBP-1. Immunohistochemical reactivity for HBp17/FGFBP-1 was mainly observed in the membrane and cytoplasm of the peripheral/basal cells, in the squamous cells as well as in the stellate reticulum-like cells. The strongest staining intensity was seen in the squamous cells and in the peripheral/basal cells. 2A: Follicular pattern, 2B: Plexiform pattern. (x200); 2C: Follicular pattern, 2D: Plexiform pattern. (x400).

Figure 3: Immunohistochemical staining for FGF-1.

Immunohistochemical reactivity for FGF-1 was mainly observed in the squamous cells and in the cytoplasm of the peripheral/basal cells with some FGF-1-positive cells expanding into the stellate reticulum-like cell areas. Squamous cells and peripheral/basal cells exhibited strong staining intensity. 3A: Follicular pattern, 3B: Plexiform pattern. (x200); 3C: Follicular pattern, 3D: Plexiform pattern. (x400).

Figure 4: Immunohistochemical staining for FGF-2.

The expression of FGF-2 in ameloblastoma was mainly detected in the membrane and in the cytoplasm of the peripheral/basal cells as well as in the squamous cells with some FGF-2-positive cells spreading to the stellate reticulum-like cells. The stellate reticulum like cells areas were found weaker staining intensity compare to those in squamous cells and in the peripheral/basal cells areas. 4A: Follicular pattern, 4B: Plexiform pattern. (x200); 4C: Follicular pattern, 4D: Plexiform pattern. (x400).

Figure 5: Immunohistochemical staining for CD34.

Tumor microvessels with strong staining intensity of CD34 in the endothelial cells showed slightly irregular shaped, tortuous and dilated form in the stroma (Figure 5A, 5B, 5C, 5D). Follicular patterns (Figure 5A, 5C) showed many small microvessels with slightly irregular shape, whereas microvessels in plexiform patterns were scattered with dilated shape (Figure 5B, 5D). 5A: Follicular pattern, 5B: Plexiform pattern. (x200); 5C: Follicular pattern, 5D: Plexiform pattern. (x400).

Figure 6: Immunohistochemical staining for p53.

The immunohistochemical reactivity for p53 was detected in the nuclei of peripheral/basal cells with some p53-positive cells spreading to the stellate reticulum-like cells. The p53-positive cells in the reticulum-like cell area showed lower intensity than that in the peripheral/basal cell area. 6A: Follicular pattern, 6B: Plexiform pattern. (x200); 6C: Follicular pattern, 6D: Plexiform pattern. (x400).

Figure 7: Immunohistochemical staining for pRB.

Immunohistochemical reactivity for pRB in ameloblastomas was mainly observed in the nuclei of the tumor cells. The pRB-positive cells in the peripheral/basal areas exhibited stronger staining intensity than those in the stellate reticulum-like areas. 7A: Follicular pattern, 7B: Plexiform pattern. (x200); 7C: Follicular pattern, 7D: Plexiform pattern. (x400).

Figure 8: Immunohistochemical staining for Ki67.

The expression of Ki67 protein in ameloblastomas was observed in nuclei of tumor cells with strong immunostaining intensity. A few scattered Ki67-positive cells were observed in the peripheral/basal cells and occasionally seen in the stellate reticulum-like cells. There is no significant difference in an intensity of Ki67-positive cells between in the stellate reticulum-like cell area and in the

peripheral/basal cell area. 8A: Follicular pattern, 8B: Plexiform pattern. (x200); 8C: Follicular pattern, 8D: Plexiform pattern. (x400).

Figure 9: Double Ki67-CD34 antigens staining.

Follicular patterns where tumor islands with high expression of Ki67 showed many small microvessels with irregular shape (Figure 9A, 9B) whereas plexiform patterns where tumor islands with high expression of Ki67 showed few microvessels with dilated shape (Figure 9C, 9D). 9A: Follicular pattern, 9B: Plexiform pattern. (x200); 9C: Follicular pattern, 9D: Plexiform pattern. (x400).

Figure 10: Scatter plots showing the correlation between Ki67 and p53

10A: No correlation between the Ki67 LI and p53 LI.

10B: Correlation between the Ki67 dEI and p53 dEI. Correlation lines with asterisk * showing the significant correlation between p53 and Ki67 (blue line).

Figure 11: Scatter plots showing the correlation between pRB and Ki67, p53. 11A: Correlation between the pRB LI and Ki67 LI, p53 LI. Correlation lines with asterisk * showing the significant correlation between pRB LI and Ki67 LI (red line), p53 LI (blue line). 11B: Correlation between the pRB dEI and Ki67 dEI, p53 dEI. Correlation lines with asterisk * showing the significant correlation between pRB dEI and Ki67 dEI (red line), p53 dEI (blue line).

Figure 12: Scatter plots showing the correlation between Ki67 and microvessel. 12A: No correlation between the expression of Ki67 and MVD. 12B: Correlation between the expression of Ki67 and pTS. Correlation lines with asterisk * showing the significant correlation between pTS and Ki67 LI (blue line), Ki67 dEI (red line).

Figure 13: Scatter plots showing the correlation between HBp17/FGFBP-1 and FGF-1, FGF-2, microvessels.

13A: Correlation between the HBp17/FGFBP-1 dEI and FGF-1 dEI, FGF-2 dEI. Correlation lines with asterisk * showing the significant correlation between HBp17/FGFBP-1 dEI and FGF-1 dEI (red line), FGF-2 dEI (blue line). 13B: Correlation between the HBp17/FGFBP-1 dEI and MVD, pTS. Correlation lines with asterisk * showing the significant correlation between HBp17/FGFBP-1 dEI and MVD (red line), pTS (blue line)

Figure 14: Scatter plots showing the correlation between Ki67 with HBp17/FGFBP-1, FGF-1, FGF-2.

The correlation lines with asterisk * showing the significant correlation between Ki67 dEI and HBp17/FGFBP-1 dEI (green line), FGF-1 dEI (blue line), FGF-2 dEI (red line).

Figure 15: Scatter plots showing the correlation between p53 and HBp17/FGFBP-1, FGF-1, FGF-2, microvessels.

15A: Correlation between p53 and HBp17/FGFBP-1, FGF-1, FGF-2. Correlation lines with asterisk * showing the significant correlation between p53 dEI and HBp17/FGFBP-1 dEI (green line), FGF-1 dEI (red line), FGF-2 dEI (blue line). 15B: Correlation between p53 and MVD, pTS. Correlation lines with asterisk * showing the significant correlation between p53 dEI and MVD (red line), pTS (blue line).

Figure 16: Scatter plots showing the correlation between the estimated tumor volume and the expression of HBp17/FGFBP-1, pRB.

The correlation lines with asterisk * showing the significant correlation between the estimated tumor volume and HBp17/FGFBP-1 dEI (blue line), pRB dEI (red line).

Tables

Table 1: Primary antibody and Secondary antibody

Primary antibody	Secondary antibody
Monoclonal Mouse IgG1 anti HBp17/FGFBP-1 antibody (MAB1593, R&D systems, Minneapolis, USA, diluted 1:100)	Goat anti Mouse IgG (H+L) – HRP (Bio-Rad Laboratories, CA, USA, diluted 1:100)
Polyclonal Rabbit anti FGF1 antibody (Santa Cruz, CA, diluted 1:100)	Labeled polymer-HRP anti-Rabbit (Dako, Glostrup, Denmark, Ready-to-Use)
Monoclonal Mouse anti FGF2 antibody (abcam, Tokyo, Japan, diluted 1:2000)	Labeled polymer-HRP anti-Mouse (Dako, Ready-to-Use)
Monoclonal Mouse anti CD34 class II antibody (clone QBEnd10, N1632, Dako, Ready-to-Use)	Labeled polymer-HRP anti-Mouse (Dako, Ready-to-Use)
Monoclonal Mouse anti p53 antibody (clone DO-7, M7001, Dako, diluted 1:50)	Labeled polymer-HRP anti-Mouse (Dako, Ready-to-Use)
Monoclonal Mouse anti pRB antibody (Rb (IF8): sc-102, Santa Cruz, diluted 1:100)	Labeled polymer-HRP anti-Mouse (Dako, Ready-to-Use)
Monoclonal Mouse anti Ki67 antibody (clone MIB-1, M7240, Dako, diluted 1:100)	Labeled polymer-HRP anti-Mouse (Dako, Ready-to-Use)

Table 2: Samples of study

Gender	SMA	UA	DA	EA	Malignant ameloblastoma	Ameloblastic carcinoma
15 Men	11	3	0	0	0	1
16 Women	12	3	0	0	0	1

Table 3 A, B: Correlation between p53, pRB and Ki67. Spearman's rank correlation test, asterisk * indicates the significant correlation (2-tailed) ($p<0.05$).

Table 3A: Correlation between p53 LI, pRB LI and Ki67 LI. The asterisk * indicates the significant correlation (2-tailed) ($p<0.05$).

Spearman's rho		pRB LI	P53 LI	Ki67 LI
pRB LI	Correlation Coefficient	1	0.867*	0.537*
	Sig. (2-tailed)		<0.001	0.003
	N	29	29	29
P53 LI	Correlation Coefficient	0.867*	1	0.317
	Sig. (2-tailed)	<0.001		0.094
	N	29	29	29
Ki67 LI	Correlation Coefficient	0.537*	0.317	1
	Sig. (2-tailed)	0.003	0.094	
	N	29	29	29

Table 3B: Correlation between p53 dEI, pRB dEI and Ki67 dEI. The asterisk * indicates the significant correlation (2-tailed) ($p<0.05$).

Spearman's rho		pRB dEI	P53 dEI	Ki67 dEI
pRB dEI	Correlation Coefficient	1	0.903*	0.475*
	Sig. (2-tailed)		<0.001	0.009
	N	29	29	29
P53 dEI	Correlation Coefficient	0.903*	1	0.431*
	Sig. (2-tailed)	<0.001		0.02
	N	29	29	29
Ki67 dEI	Correlation Coefficient	0.475*	0.431*	1
	Sig. (2-tailed)	0.009	0.02	
	N	29	29	29

Table 4: Correlation between Ki67 and MVD, pTS. The asterisk * indicates the significant correlation (2-tailed) ($p<0.05$).

Spearman's rho		MVD	pTS
Ki67 LI	Correlation Coefficient	0.27	0.588*
	Sig. (2-tailed)	0.157	0.001
	N	29	29
Ki67 dEI	Correlation Coefficient	0.234	0.545*
	Sig. (2-tailed)	0.221	0.002
	N	29	29

Table 5: Correlation between HBp17/FGFBP-1 dEI, FGF-1 dEI, FGF-2 dEI and MVD, pTS. Spearman's rank correlation test, asterisk * indicates the significant correlation at the 0.001 level (2-tailed) ($p<0.05$).

Spearman's rho		HBp17/	FGF-1	FGF-2
HBp17/ FGFBP-1 dEI	Correlation Coefficient	1	0.737*	0.803*
	Sig. (2-tailed)		<0.001	<0.001
	N	29	29	29
FGF-1 dEI	Correlation Coefficient	0.737*	1	0.606*
	Sig. (2-tailed)	<0.001		<0.001
	N	29	29	29
FGF-2 dEI	Correlation Coefficient	0.803*	0.606*	1
	Sig. (2-tailed)	<0.001	<0.001	
	N	29	29	29
MVD	Correlation Coefficient	0.662*	0.759*	0.713*
	Sig. (2-tailed)	<0.001	<0.001	<0.001
	N	29	29	29
pTS	Correlation Coefficient	0.784*	0.716*	0.913*
	Sig. (2-tailed)	<0.001	<0.001	<0.001
	N	29	29	29
Ki67 dEI	Correlation Coefficient	0.559*	0.514*	0.387*
	Sig. (2-tailed)	0.002	0.004	0.038
	N	29	29	29

Table 6: The correlation with age. Kruskal-Wallis test. The asterisk * indicates the significant correlation (2-tailed) ($p<0.05$).

	Age	N	Mean Rank	Asym. Sig (2-tailed)
HBp17/FGFBP-1 LI	<20	5	9.80	0.340
	20-40	17	15.00	
	>40	7	18.71	
FGF-1 LI	<20	5	13.00	0.564
	20-40	17	14.41	
	>40	7	17.86	
FGF-2 LI	<20	5	11.00	0.445
	20-40	17	15.24	
	>40	7	17.29	
p53 LI	<20	5	10.06	0.122
	20-40	17	14.12	
	>40	7	20.29	
pRB LI	<20	5	7.60	0.031*
	20-40	17	14.82	
	>40	7	20.71	
Ki67 LI	<20	5	11.40	0.240
	20-40	17	17.24	
	>40	7	12.14	

(to be continued)

	Age	N	Mean Rank	Asym. Sig (2-tailed)
HBp17/FGFBP-1 dEI	<20	5	9.00	0.181
	20-40	17	15.53	
	>40	7	18	
FGF-1 dEI	<20	5	12.00	0.489
	20-40	17	14.71	
	>40	7	17.86	
FGF-2 dEI	<20	5	13.00	0.537
	20-40	17	14.35	
	>40	7	18.00	
MVD	<20	5	11.60	0.587
	20-40	17	15.35	
	>40	7	16.57	
pTS	<20	5	12.60	0.694
	20-40	17	14.94	
	>40	7	16.86	
p53 dEI	<20	5	9.80	0.192
	20-40	17	14.96	
	>40	7	18.86	
pRB dEI	<20	5	8.60	0.049*
	20-40	17	14.53	
	>40	7	20.71	
Ki67 dEI	<20	5	12.00	0.261
	20-40	17	17.18	
	>40	7	11.86	

Table 7: The correlation of these factors between SMA and UA. Mann-Whitney U test. The asterisk * indicates the significant correlation (2-tailed) ($p<0.05$).

	Subtype	N	Mean Rank	Asym. Sig (2-tailed)
HBp17/FGFBP-1 LI	UA	6	12.67	0.451
	SMA	23	15.61	
FGF-1 LI	UA	6	12.83	0.484
	SMA	23	15.57	
FGF-2 LI	UA	6	12.00	0.333
	SMA	23	15.78	
p53 LI	UA	6	8.50	0.036*
	SMA	23	16.70	
pRB LI	UA	6	10.17	0.118
	SMA	23	16.26	
Ki67 LI	UA	6	15.17	0.957
	SMA	23	14.96	

(to be continued)

	Subtype	N	Mean Rank	Asym. Sig (2-tailed)
HBp17/FGFBP-1 dEI	UA	6	13.50	0.628
	SMA	23	15.39	
FGF-1 dEI	UA	6	14.00	0.747
	SMA	23	15.26	
FGF-2 dEI	UA	6	11.33	0.236
	SMA	23	15.96	
MVD	UA	6	13.17	0.554
	SMA	23	15.48	
pTS	UA	6	12.50	0.419
	SMA	23	15.65	
p53 dEI	UA	6	10.83	0.178
	SMA	23	16.09	
pRB dEI	UA	6	10.33	0.132
	SMA	23	16.22	
Ki67 dEI	UA	6	15.17	0.957
	SMA	23	14.96	

Table 8: The expression of HBp17/FGFBP-1, FGF-1, FGF-2, MVD, pTS, p53, pRB, Ki67 in benign ameloblastoma (mean± SD) and in ameloblastic carcinoma

Factors	Benign ameloblastomas (Mean± SD)	Ameloblastic Carcinoma
HBp17/FGFBP-1 LI	34.99±19.57	53.75
HBp17/FGFBP-1 dEI	21.98±14.96	44.71
FGF-1 LI	31.45±10.99	52.05
FGF-1 dEI	30.40±16.57	38.68
FGF-2 LI	70.38±22.93	83.73
FGF-2 dEI	54.77±25.16	59.11
MVD	64.25±23.70	77.80
pTS	36.87±18.79	37.63
p53 LI	29.16±12.80	51.56
p53 dEI	36.87±17.47	71.91
pRB LI	32.06±20.30	77.37
pRB dEI	44.52±37.08	138.56
Ki67 LI	4.32±4.05	2.51
Ki67 dEI	8.16±7.94	4.42

Figures

Figure 1: Hematoxylin and Eosin staining.

1A: Follicular pattern, 1B: Plexiform pattern. (x200).

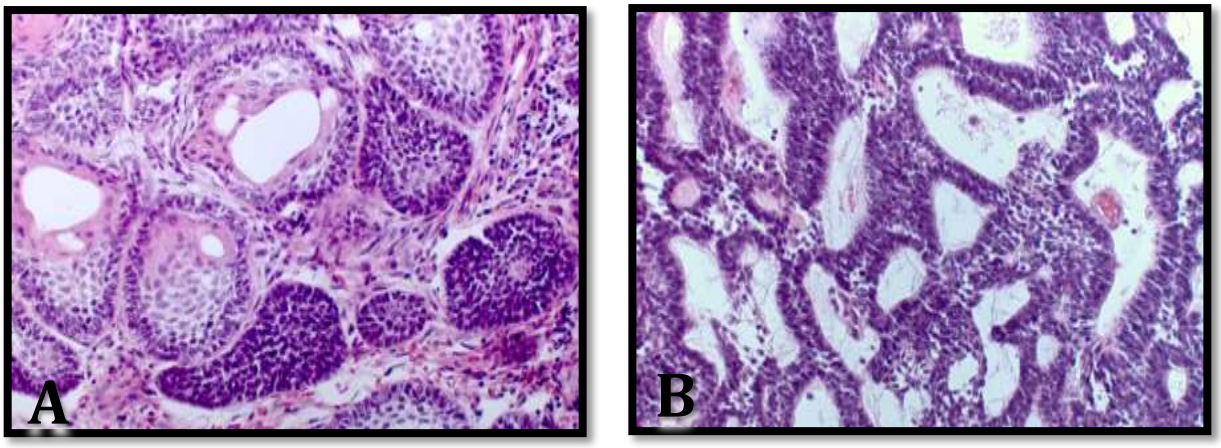

Figure 2: Immunohistochemical reactivity for HBp17/FGFBP-1.

2A: Follicular pattern, 2B: Plexiform pattern (x200)

2C: Follicular pattern, 2D: Plexiform pattern (x400).

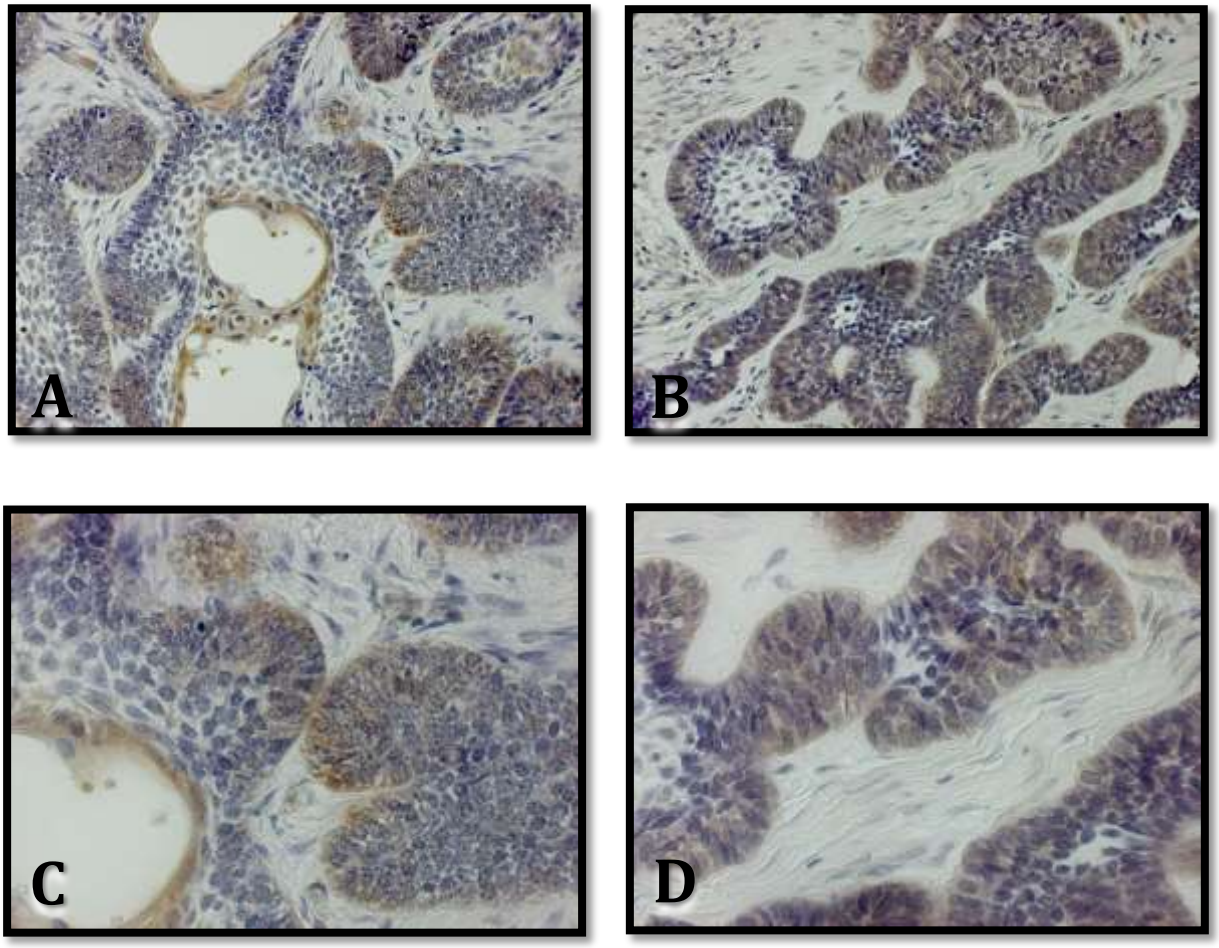

Figure 3: Immunohistochemical reactivity for FGF-1.

3A: Follicular pattern, 3B: Plexiform pattern (x200).

3C: Follicular pattern, 3D: Plexiform pattern (x400).

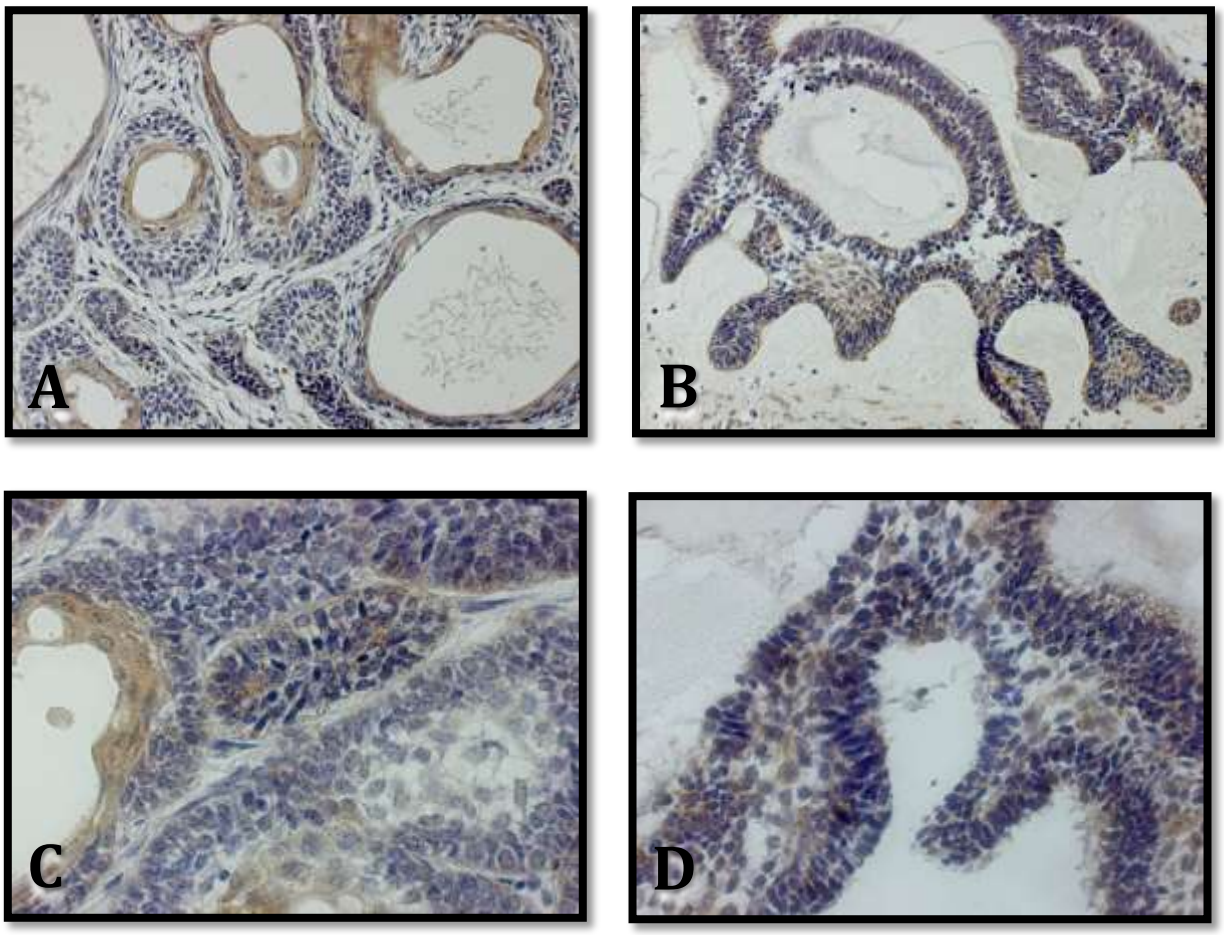

Figure 4: Immunohistochemical reactivity for FGF-2.

4A: Follicular pattern, 4B: Plexiform pattern. (x200)

4C: Follicular pattern, 4D: Plexiform pattern. (x400)

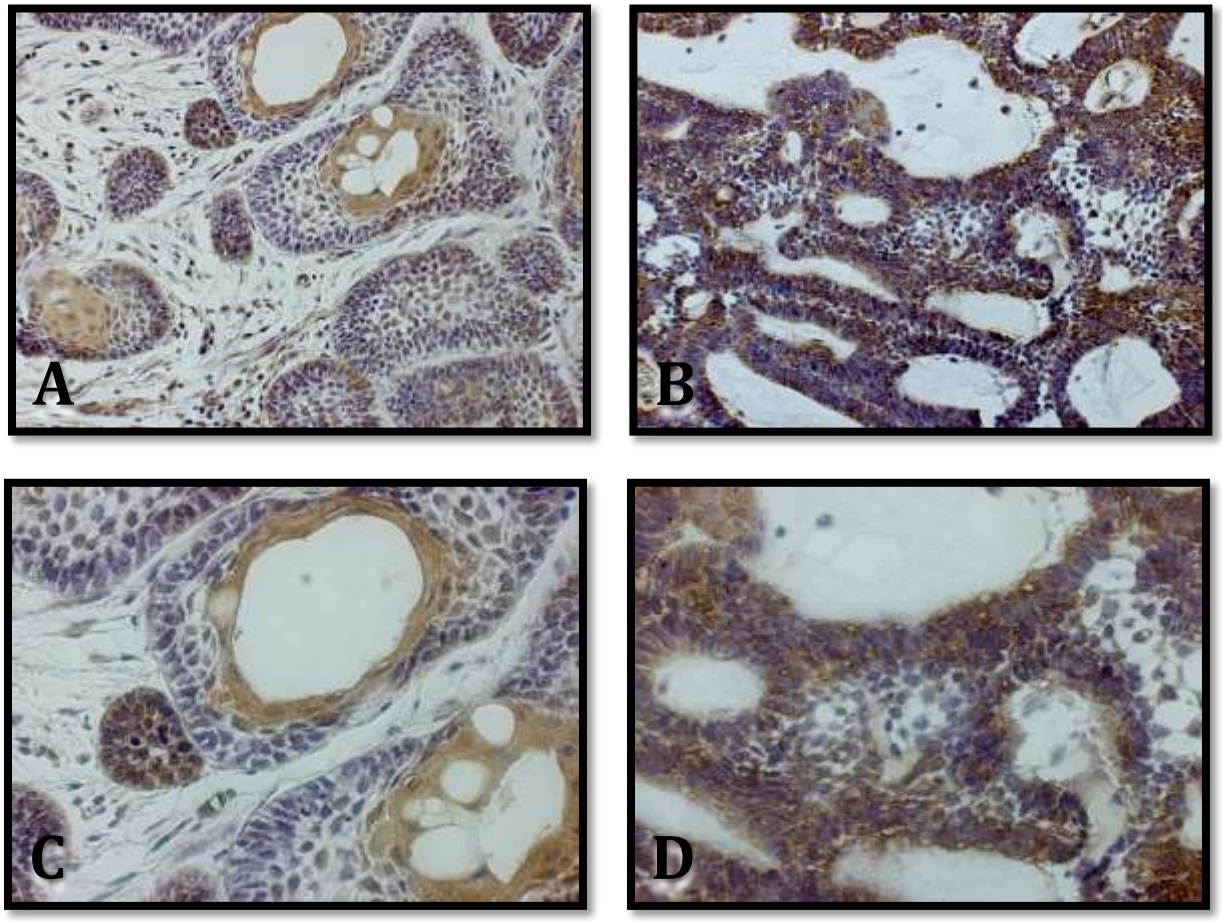

Figure 5: Immunohistochemical staining for CD34.

5A: Follicular pattern, 5B: Plexiform pattern. (x200)

5C: Follicular pattern, 5D: Plexiform pattern. (x400)

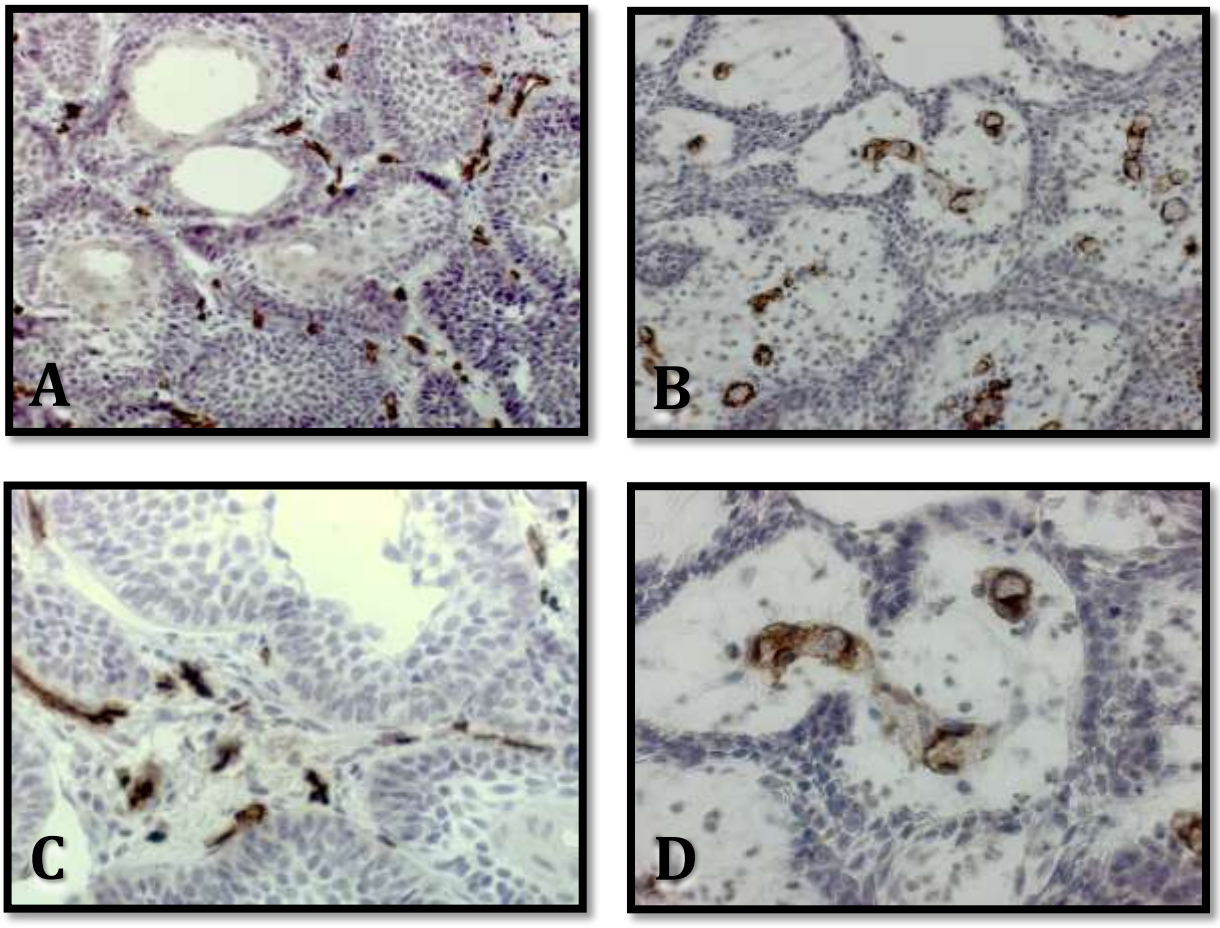

Figure 6: Immunohistochemical staining for p53.

6A: Follicular pattern, 6B: Plexiform pattern (x200).

6C: Follicular pattern, 6D: Plexiform pattern (x400).

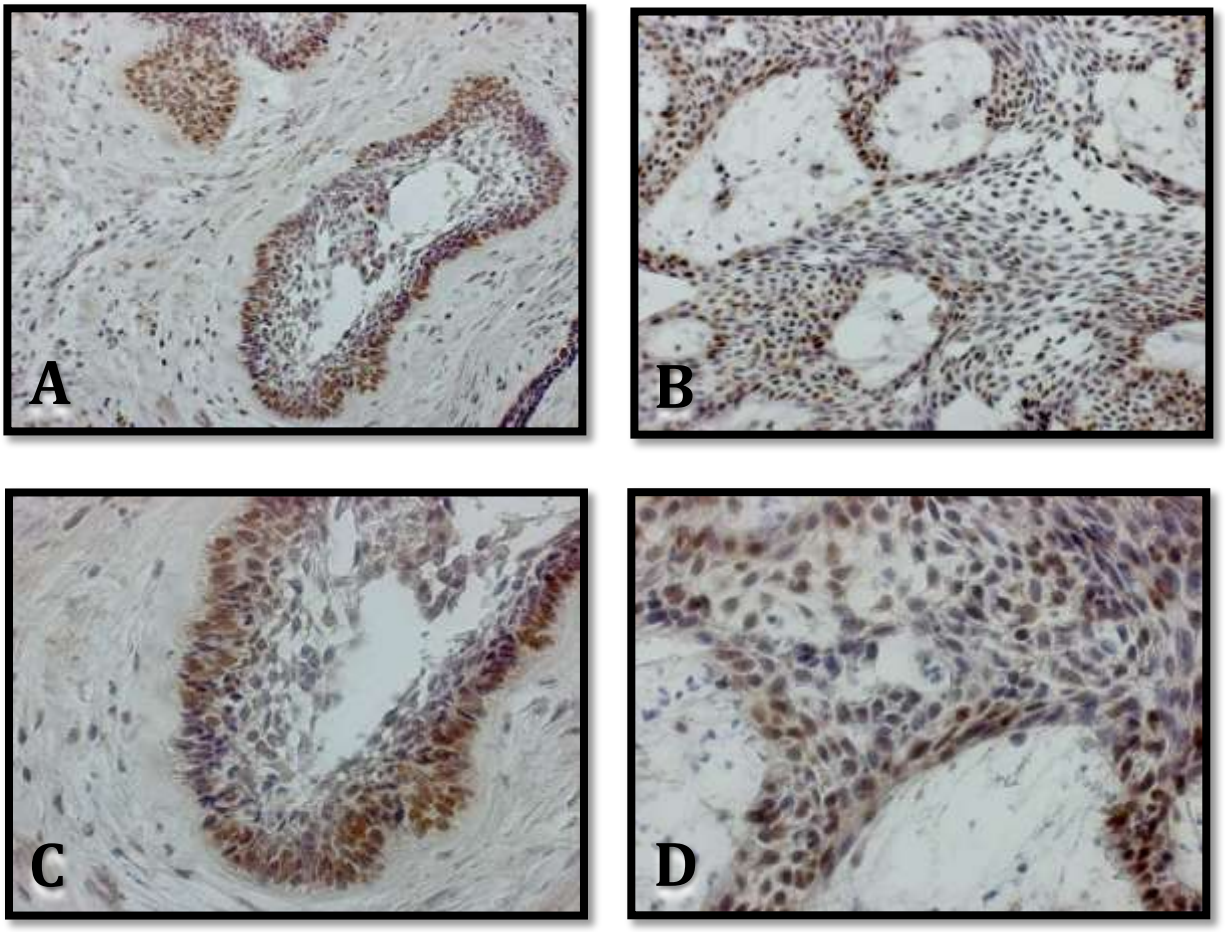

Figure 7: Immunohistochemical staining for pRB.

7A: Follicular pattern, 7B: Plexiform pattern. (x200).

7C: Follicular pattern, 7D: Plexiform pattern. (x400).

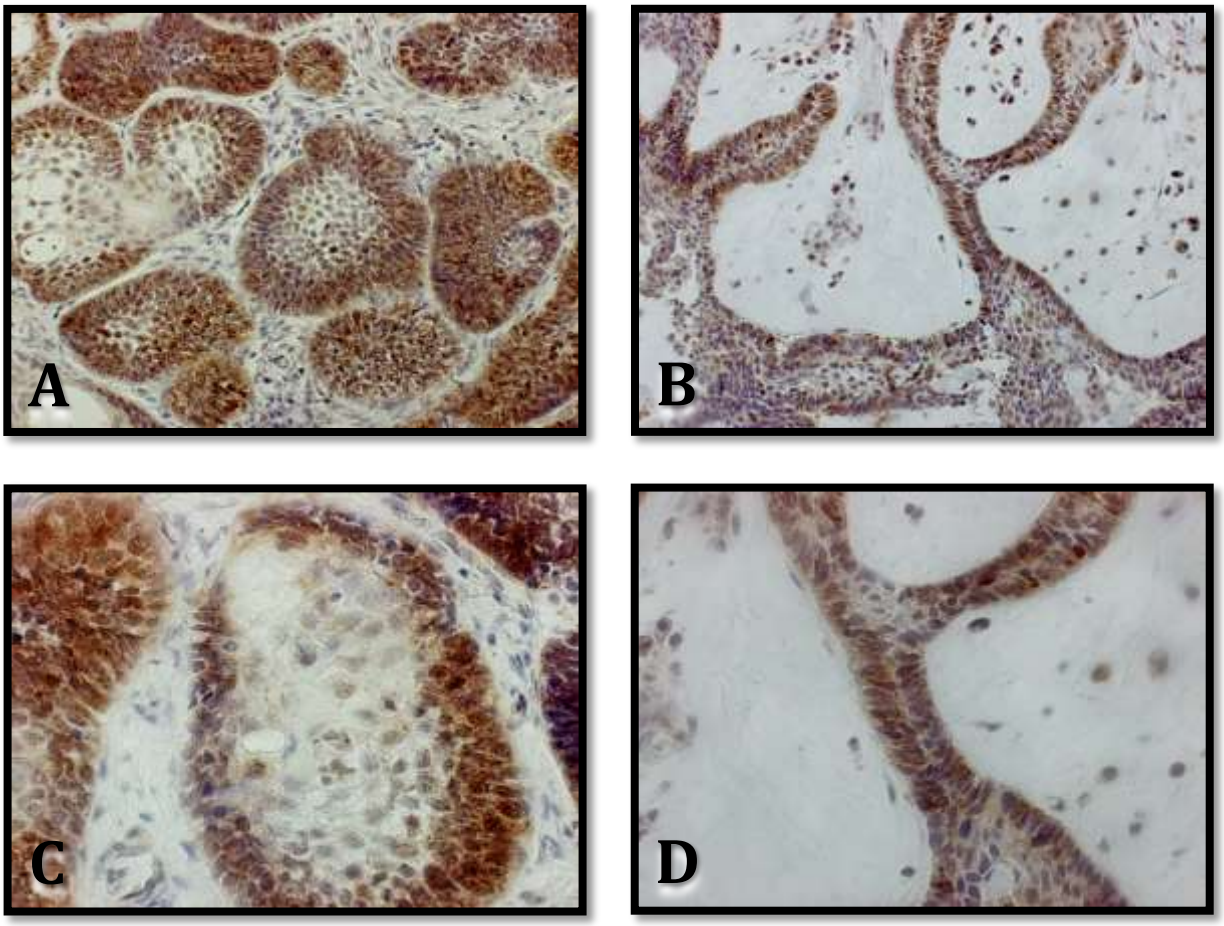

Figure 8: Immunohistochemical staining for Ki67.

8A: Follicular pattern, 8B: Plexiform pattern. (x200).

8C: Follicular pattern, 8D: Plexiform pattern. (x400).

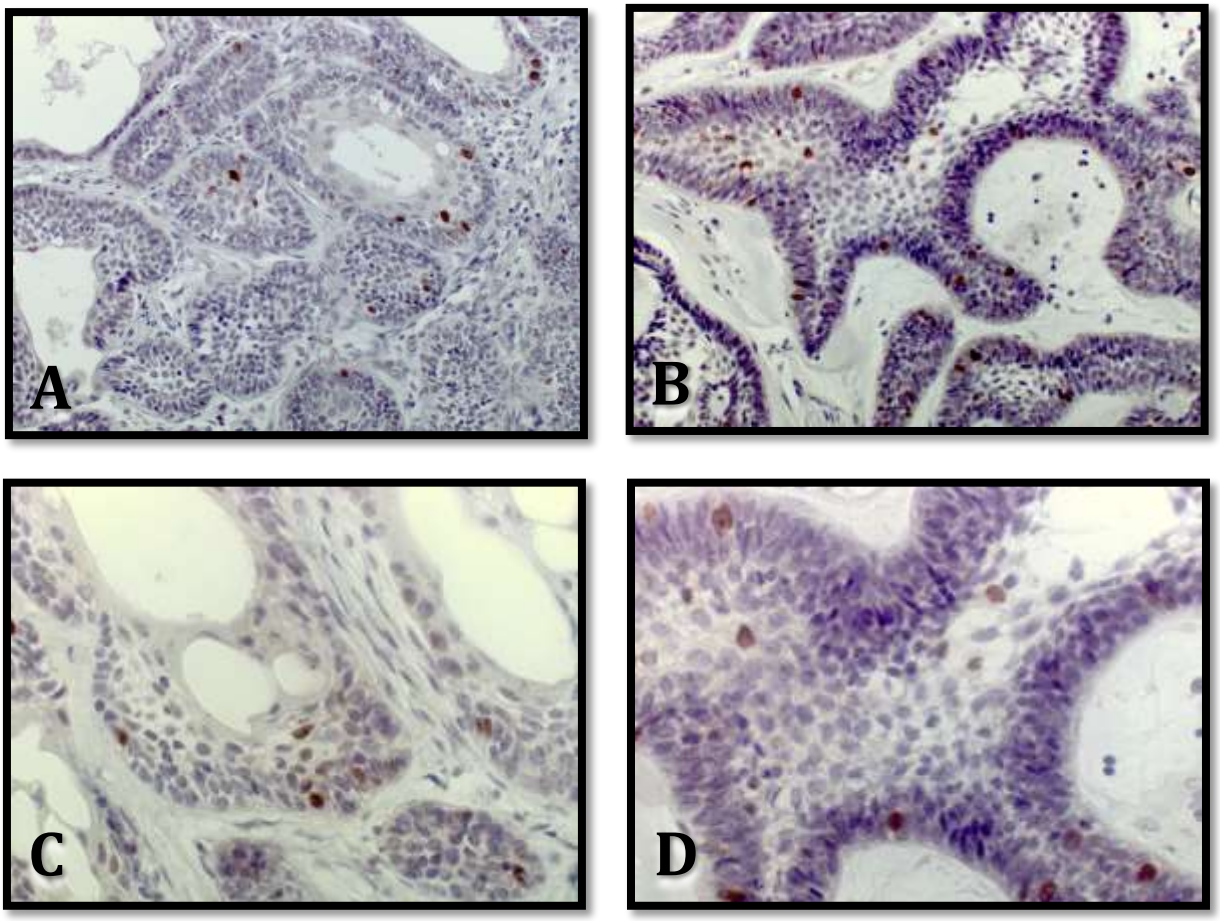

Figure 9: Double Ki67-CD34 antigens staining.

9A: Follicular pattern, 9B: Plexiform pattern. (x200).

9C: Follicular pattern, 9D: Plexiform pattern. (x400).

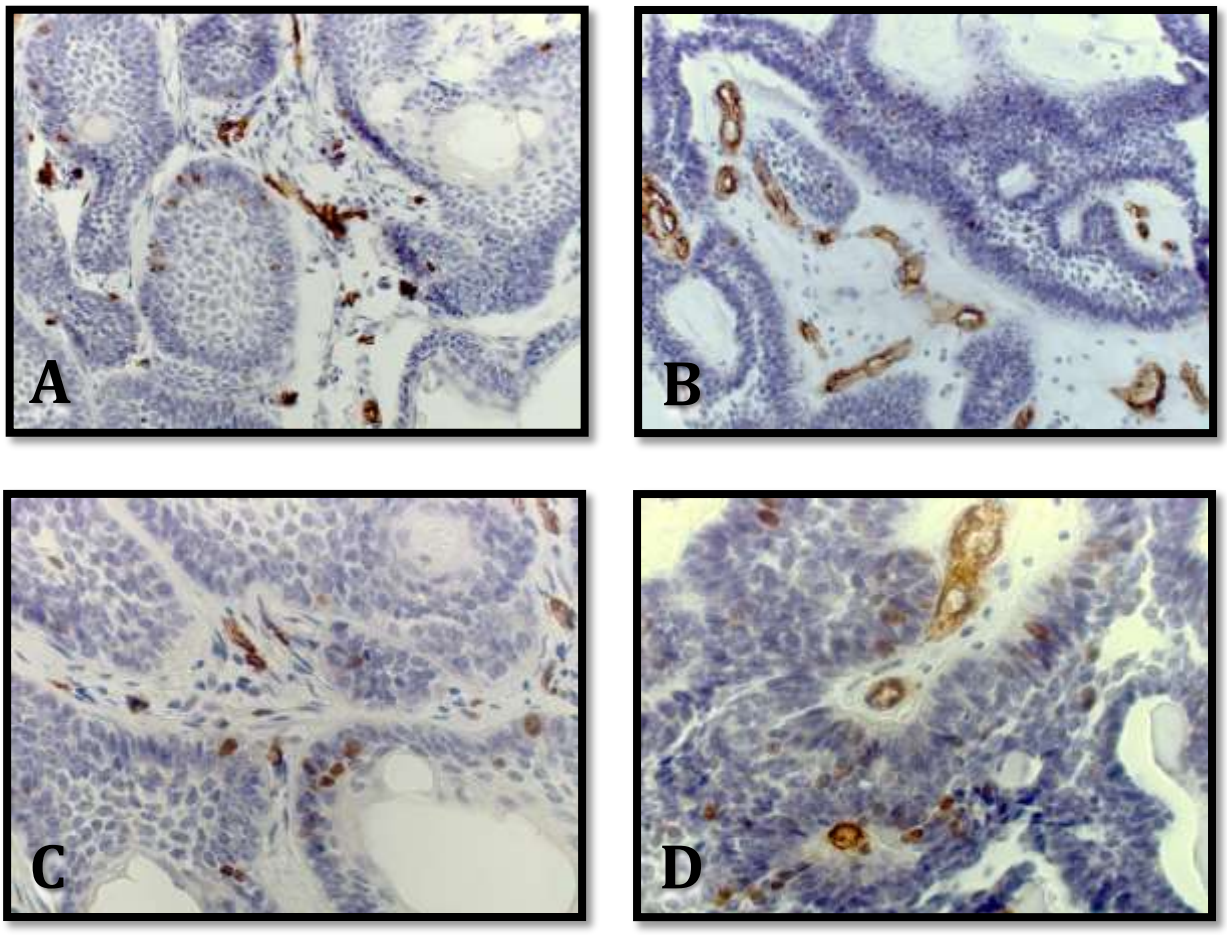

Figure 10: Scatter plots showing the correlation between Ki67 and p53

10 A: No correlation between the Ki67 LI and p53 LI.

10 B: Correlation between the Ki67 dEI and p53 dEI. The correlation lines with asterisk * showing the significant correlation between p53 and Ki67 (blue line).

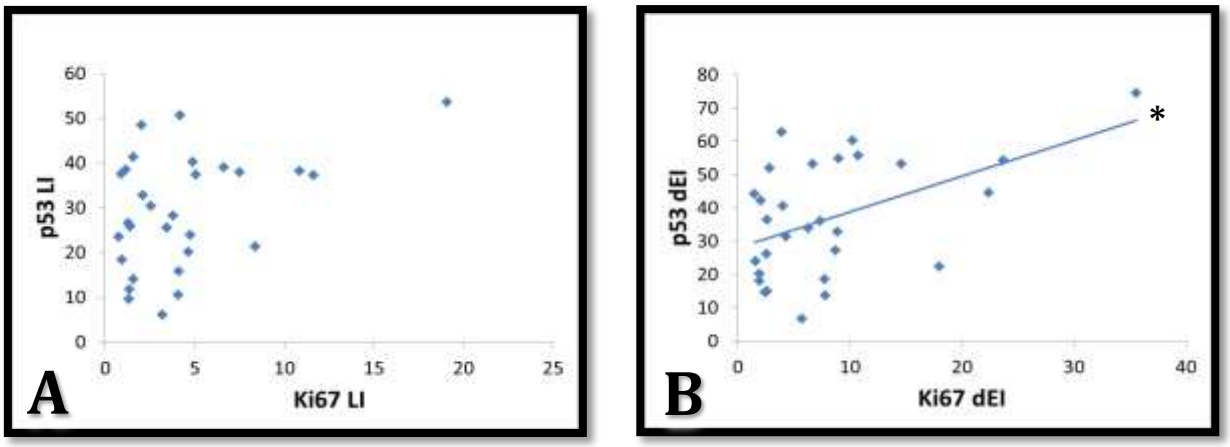

Figure 11: Scatter plots showing the correlation between pRB and Ki67, p53.

11 A: Correlation between the pRB LI and Ki67 LI, p53 LI. The correlation lines with asterisk * showing the significant correlation between pRB LI and Ki67 LI (red line), p53 LI (blue line). 11 B: Correlation between the pRB dEI and Ki67 dEI, p53 dEI. The correlation lines with asterisk * showing the significant correlation between pRB dEI and Ki67 dEI (red line), p53 dEI (blue line).

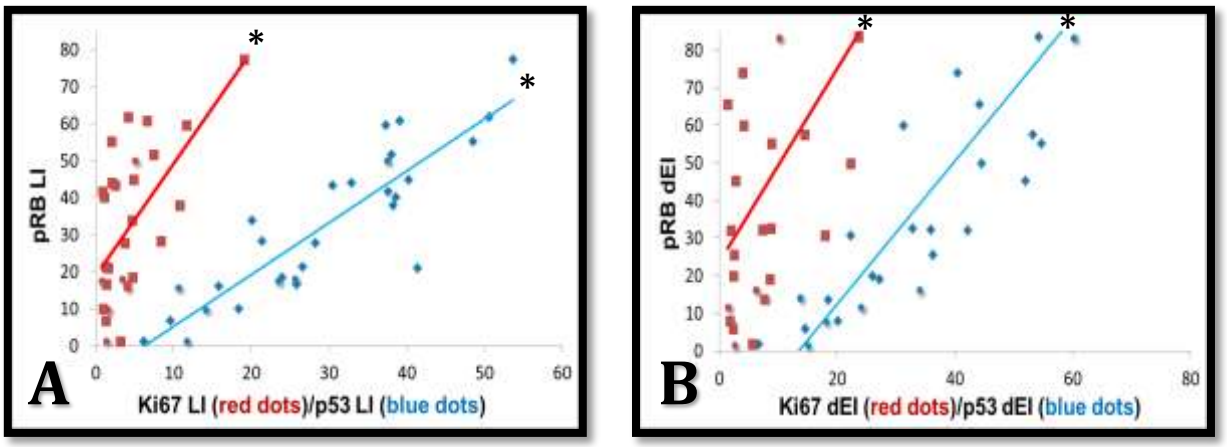

Figure 12: Scatter plots showing the correlation between Ki67 and microvessel. 12 A: No correlation between the expression of Ki67 and MVD. 12 B: Correlation between the expression of Ki67 and pTS. The correlation lines with asterisk * showing the significant correlation between pTS and Ki67 LI (blue line), Ki67 dEI (red line).

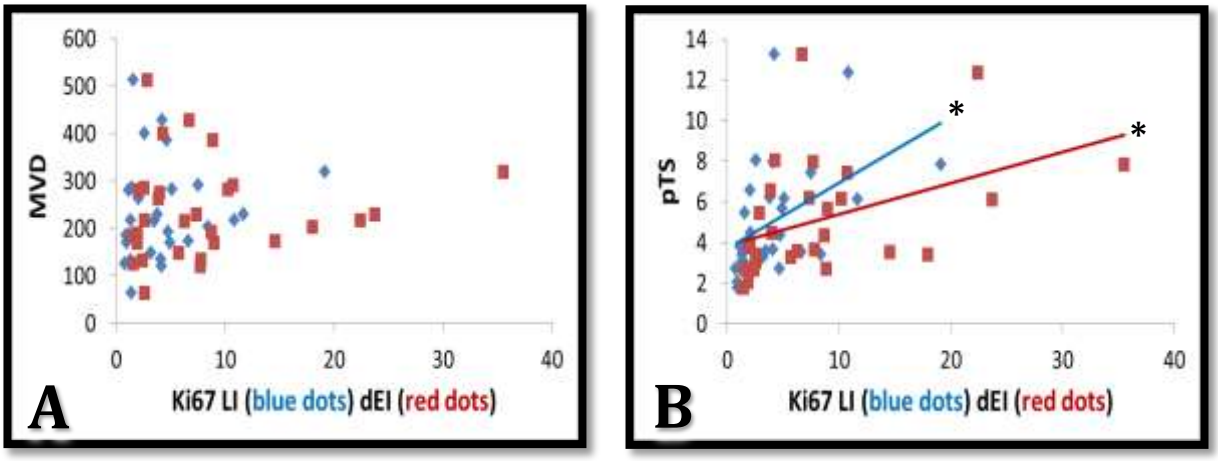

Figure 13: Scatter plots showing the correlation between HBp17/FGFBP-1 and FGF-1, FGF-2, microvessels. 13 A: Correlation between the HBp17/FGFBP-1 dEI and FGF-1 dEI, FGF-2 dEI. The correlation lines with asterisk * showing the significant correlation between HBp17/FGFBP-1 dEI and FGF-1 dEI (red line), FGF-2 dEI (blue line). 13 B: Correlation between the HBp17/FGFBP-1 dEI and MVD, pTS. The correlation lines with asterisk * showing the significant correlation between HBp17/FGFBP-1 dEI and MVD (red line), pTS (blue line)

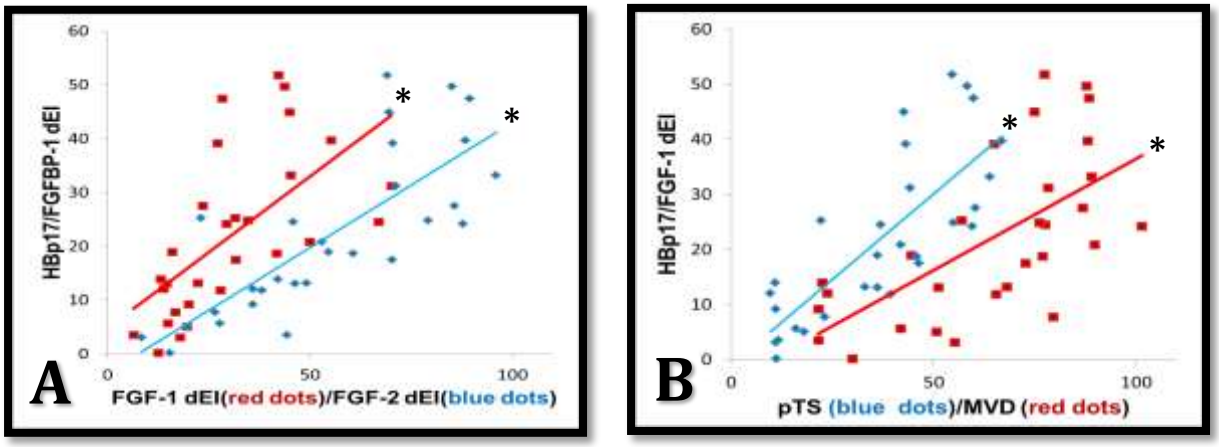

Figure 14: Scatter plots showing the correlation between Ki67 with HBp17/FGFBP-1, FGF-1, FGF-2. The correlation lines with asterisk * showing the significant correlation between Ki67 dEI and HBp17/FGFBP-1 dEI (green line), FGF-1 dEI (blue line), FGF-2 dEI (red line).

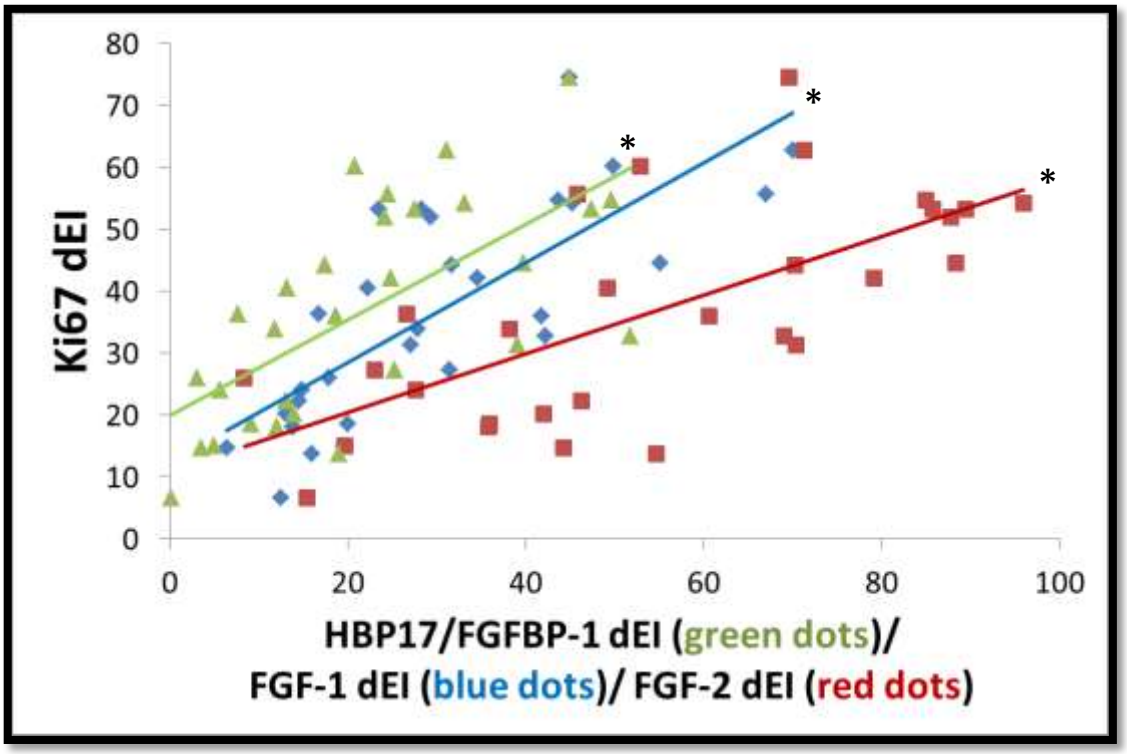

Figure 15: Scatter plots showing the correlation between p53 and HBp17/FGFBP-1, FGF-1, FGF-2, microvessels. 15 A: Correlation between p53 and HBp17/FGFBP-1, FGF-1, FGF-2. The correlation lines with asterisk * showing the significant correlation between p53 dEI and HBp17/FGFBP-1 dEI (green line), FGF-1 dEI (red line), FGF-2 dEI (blue line). 15 B: Correlation between p53 and MVD, pTS. The correlation lines with asterisk * showing the significant correlation between p53 dEI and MVD (red line), pTS (blue line).

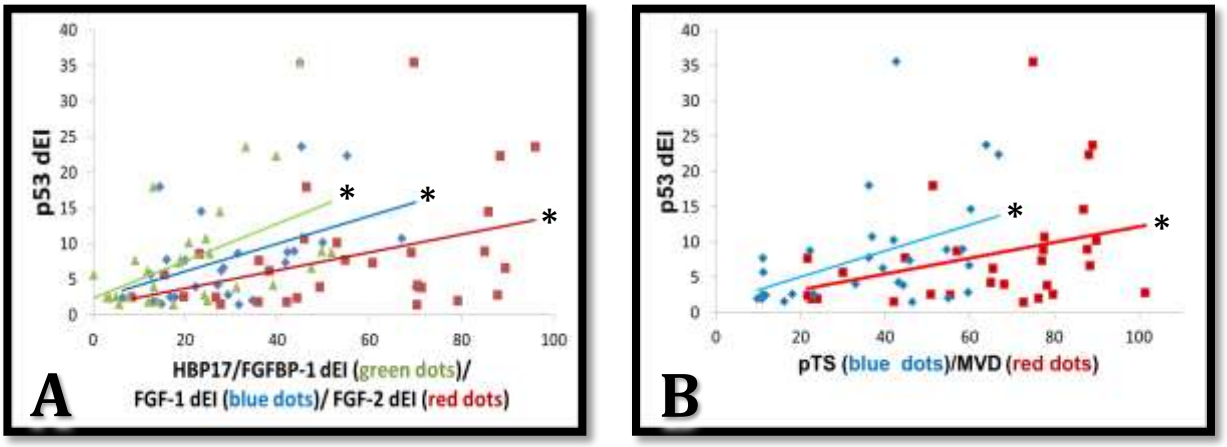

Figure 16: Scatter plots showing the correlation between the estimated tumor volume and the expression of HBp17/FGFBP-1, pRB. The correlation lines with asterisk * showing the significant correlation between the estimated tumor volume and HBp17/FGFBP-1 dEI (blue line), pRB dEI (red line).